General isotropic micropolar fluid model in smoothed particle hydrodynamics

A. Souto-Iglesias *
CEHINAV, DACSON, ETSIN, Universidad Politécnica de Madrid, Madrid, Spain

J. Bonet Avalos
Department d'Enginyeria Química, ETSEQ, Universitat Rovira i Virgili, Tarragona, Spain

M. Antuono and A. Colagrossi
CNR-INM, Institute of Marine Engineering, Rome, Italy

(Received 27 April 2021; accepted 9 July 2021; published 29 July 2021)

The smoothed particle hydrodynamics (SPH) method is used in this paper to model micropolar fluids, with emphasis on their dissipation mechanisms. To this aim, a dissipation function is defined at the particle level which depends on the relative velocity between particles but also on an additional spin degree of freedom, which modifies such relative velocity as well as introduces spin-related intrinsic dissipation mechanisms, comparable to those related to the rate of deformation tensor in Newtonian fluids. This dissipation function is then incorporated within the Lagrangian formalism, leading to a set of SPH particle equations to describe the dynamics. A continuous integral SPH version of the scheme is obtained with a bottom-up derivation which guarantees the consistency of the SPH term. The model is then enriched with two additional terms based exclusively on the spin derivatives, which grant it the maximal generality as an isotropic model for micropolar fluids. Finally, numerical verification and validation tests are documented that show that SPH is capable of accurately modeling this type of dynamics.

DOI: 10.1103/PhysRevE.104.015315

I. INTRODUCTION

Smoothed Particle Hydrodynamics (SPH) is a numerical technique that can simulate macroscopic flows through a Lagrangian description of the fluid dynamics [1,2]. In regard to the application of the method to different types of fluids, as expected due to their prevalence, Newtonian fluids have received much attention (see, e.g., Refs. [3–6]). Beyond, there have been successful attempts to model more complex fluids with SPH, such as, e.g., Oldroyd type [7–10], Jaumann-Maxwell [11], and inelastic non-Newtonian [12]. Such attempts have been complemented by the addition of thermal fluctuations to the SPH model to describe mesoscopic scales (known as SDPD), which allowed to model polymer molecules in suspension [13,14] and blood flow [15]. As the complexity of the fluid behavior increases, there is major concern about how the extensions of the SPH method affect fundamental aspects of fluid motion, such as the conservation of linear and angular momentum, and any other property inherited from the underlying microscopic physical reality.

In Refs. [16,17], the introduction of dissipation functions at the particle level, with the appropriate symmetries related to Galilean invariance, rotational invariance and tensorial objectiveness [18], allowed us to derive the SPH form of the Newtonian viscous terms from first principles of conservation and thermodynamic consistency. This bottom-up approach is proven capable of producing new force terms to model an arbitrary bulk viscosity, independent of the shear viscosity, the latter modeled through the usual Monaghan and Gingold's term [19], for example. The objective of present research is to apply this technique to derive SPH equations for more complex fluids, in particular micropolar ones, with the maximal generality. The application of this method, in addition, has allowed us to critically review some of the existent approaches within the SPH framework, which is also of physical interest.

Micropolar fluids are fluids with microstructure, reflected in these fluids having an additional local degree of freedom, the spin, for which a time evolution equation can be set, evolution which affects the dissipation characteristics of the flow. The polarity refers to the fact that the spin dynamics is connected to the presence of torques at the microscopic level. The reader is referred to references [18,20–22] for extensive descriptions of the physical models for these fluids. In regards to their practical applications, a review is provided by Ariman *et al.* [23]. Lubrication modeling appears as an important area because the presence of additives and dirt in the lubricating fluids deviates their physical behavior from the Newtonian model [24]. More recently, even this kind of microrotation related diffusion processes has been investigated in the context of the transport of coronavirus in body fluids [25].

Even though the nature of micropolar fluids seems to intrinsically match with the basis of a particle method such as SPH, they have scarcely been treated in the SPH literature. In the context of computer graphics, a number of authors have recently incorporated a spin degree of freedom to their SPH

*antonio.souto@upm.es

model, with the aim of tuning the intensity of turbulent structures [26–30]. In SDPD, analogous to SPH but with thermal fluctuations, Müller *et al.* [31], inspired by previous works in the Voronoi particle dynamics method [32], incorporated a spin degree of freedom to construct a model in which the angular momentum is conserved despite the fact that the forces between particles are not central, i.e., torques are exerted on the particles. An example of noncentral forces is the type introduced by Morris [33] for the translational motion of the particles which, if no description of the rotational dynamics is introduced, leads to the nonconservation of the total angular momentum. However, although the formulation of Müller *et al.* [31] restores the conservation of angular momentum, the dynamics of the particle spin is very restrictive, as is applicable to Newtonian fluids only.

In this article we show, in the first place, that the spin inertia is of molecular size in the continuum limit and, therefore, is negligible in most of the possible practical cases. This implies the well known result for Newtonian fluids that the particle spin follows the local vorticity and has no independent dynamics. As a consequence, the role of the spin in this SPH formulation is scale-dependent, and its importance vanishes in the continuum limit. Secondly, we propose a method to assign a moment of inertia to the model particles which reflects such scale-dependence. With this prescription, we show that the fluid conserves angular momentum even if there are noncentral interparticle forces inducing net torques. Without the explicit description of the spin, such tangential forces are forbidden if angular momentum is to be conserved, as we demonstrated [16,17].

In the third place, we generalize the spin dynamics beyond Newtonian fluids, by introducing new dissipation terms into the SPH bottom-up formulation that have not been modeled at the discrete level and validated, so far. These new terms eventually induce spatial derivatives of the spin variable in the continuum limit. Within this model, even though the moment of inertia is of molecular size (vanishingly small from the SPH perspective), still the spin is not enslaved by the vorticity, but it behaves as an independent field, coupled to the translational dynamics of the fluid. Our scheme will, by construction, conserve angular momentum, a property which is desirable in any numerical scheme, particularly if free surfaces are involved (see, e.g., Refs. [34–36]), and which has received particular attention in the SPH literature [37–39]. We show that the new terms included in the SPH description permit to model the general micropolar fluid described by the pioneering work of Condiff and Dahler [21] in the continuum limit. Therefore, the new SPH model presented in this article can be considered as the most general particulate description for micropolar fluids.

The paper is organized as follows: in Sec. II we introduce the SPH framework, and derive the new contribution to the dissipation force for a general system with an additional spin degree of freedom. The hydrodynamic limit of the model is derived in Sec. III and is shown to be equivalent to a particular micropolar fluid viscous term, which has no effect on steady-state solutions of the problem for common macroscopic fluid conditions. The model is then, in Sec. IV, enriched to account for dissipation mechanisms based on spin variations that eventually lead to a general model for micropolar fluid dynamics. Numerical verification and validation cases are proposed in Secs. V and VI. Some conclusions are enumerated and future work threads proposed to close the paper.

II. DERIVATION OF A SPH FORMULATION WITH SPIN

A. The SPH approximation to the hydrodynamic fields

Let us consider an ensemble of N isotropic particles representing fluid elements located at positions $\boldsymbol{r}_i$, $i = 1, \ldots, N$ with velocities $\boldsymbol{u}_i$, masses m_i, and volumes V_i. Since the particles are considered as macroscopic objects, we can define the internal energy per unit of mass e_i and the particle entropy per unit of mass s_i. To model micropolar fluids, we assume that the particles are isotropic but that they can rotate. The case of nonisotropic particles will be treated elsewhere. In SPH, fields are associated to corresponding physical properties carried by particles, or defined from the immediate neighborhood. The main example of the latter is the particle mass density [40]:

$$\rho_i = m_i \sum_{j=1}^{N} W(r_{ij}; h), \tag{1}$$

where W is a weight function referred to as kernel. Here, $\boldsymbol{r}_{ij} = \boldsymbol{r}_i - \boldsymbol{r}_j$ and $r_{ij} = |\boldsymbol{r}_{ij}|$. The particle volume V_i is estimated as

$$V_i = \frac{m_i}{\rho_i}. \tag{2}$$

The kernel W is a positive definite, monotonously decreasing, integrable function with a characteristic length h (see Ref. [41] for a recent discussion on the choice of kernels' characteristic length), which will be omitted in the notation where no confusion could occur. In this article, this kernel is isotropic and its volume integral is normalized, i.e.,

$$\int d\boldsymbol{r}\, W(r) = 1. \tag{3}$$

The spatial gradient of the kernel satisfies

$$\nabla_i W(r_{ij}) = \boldsymbol{e}_{ij} \frac{dW}{dr_{ij}} = -\boldsymbol{r}_{ij} F(r_{ij}) = -\nabla_j W(r_{ij}), \tag{4}$$

where $\boldsymbol{e}_{ij} = \boldsymbol{r}_{ij}/r_{ij}$ is a unit vector, and F is defined from this equation, being a positively definite function by construction.

In SPH, to reproduce smooth fields, insensitive to the underlying particulate nature of the description, it is required that $V_i \ll h^n$, i.e., that the number of particles ν in a given particle environment, determined by the range of the kernel h, must be large enough. Here n is the dimensionality of the space. Otherwise, the local fields show large fluctuations at short wavelengths of the fields, revealing the aforementioned particulate nature of the model. Moreover, to recover the hydrodynamic behavior, as described by the Navier-Stokes equation, the so-called hydrodynamic limit must be invoked [42]. The latter states that the characteristic wavelengths of the fields must be much larger than h so that spatial variations of the fields up to $O(k^2)$ are sufficient to describe the dynamics, k being the field wave number. Hence, if $L \sim 1/k$ is the characteristic length for the variation of a hydrodynamic field, then the continuous limit description should be reached when $h/L \sim kh \to 0$ with $V_i/h^n \to 0$ [43–45]. The latter limit will be discussed in the next section.

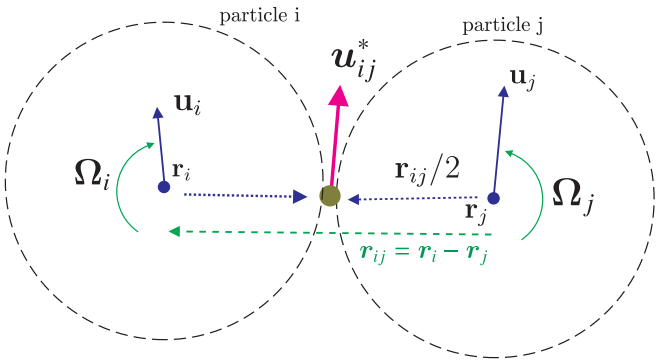

FIG. 1. Schematic representation of two interacting particles, with internal rotation, including all the variables necessary to define $\boldsymbol{u}^*_{ij}$.

Following the approach of Ref. [16], the conservative dynamics of the system can be derived from the Lagrangian

$$\mathcal{L}[\dot{\boldsymbol{r}}_i, \boldsymbol{r}_i, \dot{\boldsymbol{\theta}}_i, \boldsymbol{\theta}_i] = \sum_i \Big[\frac{1}{2}\big(m_i \dot{r}_i^2 + m_i I_i \dot{\boldsymbol{\theta}}_i^{\,2}\big) - m_i U(t, \boldsymbol{r}_i) - m_i \mathcal{V}(t, \boldsymbol{\theta}_i) - m_i e(\rho_i, s_i) \Big], \tag{5}$$

where the first term on the right-hand side of this equation is the kinetic energy of the particles, which includes a translational and a rotational term. The rotational term is computed considering an additional rotational degree of freedom, θ_i, with units of angular displacement, and the particle inertia per unit mass, I_i. In Eq. (5), U is a general external potential field such as gravity, $\mathcal{V}$ is an external potential field leading to a body torque, $\dot{\boldsymbol{r}}_i = \boldsymbol{u}_i$, and we denote $\boldsymbol{\Omega}_i = \dot{\boldsymbol{\theta}}_i$, referring to it as the *spin*, from now on. e is the internal energy, which is considered to be a function only on the particle thermodynamic properties (density, ρ_i, and entropy, s_i) in the present model.

To introduce the dissipative forces for rotating particles, let us first consider that the viscous dissipation is generated due to friction at the contact point, defined as the mid point between the centers of the two interacting particles i, and j. The composition of the translational velocity and the velocity induced by the spin (see Fig. 1) at such contact point leads to the following velocity difference at contact

$$\boldsymbol{u}^*_{ij} = \boldsymbol{u}_{ij} - \overline{\boldsymbol{\Omega}}_{ij} \times \boldsymbol{r}_{ij}, \tag{6}$$

with $\boldsymbol{u}_{ij} = \boldsymbol{u}_i - \boldsymbol{u}_j$ and $\overline{\boldsymbol{\Omega}}_{ij} := (\boldsymbol{\Omega}_i + \boldsymbol{\Omega}_j)/2$.

The assumption that the contact point can be considered as the mid point is the result of assuming that the boundaries between two adjacent particles are placed at the mid point, and therefore there is where the friction is located. Other options could be considered but one expects they would not significantly affect the long-wavelength behavior of the system.

Together with the Lagrangian, following Refs. [16,17,46] we define the dissipation function, often referred to as Rayleighian, summing all over the particles' pairs, as

$$\Phi_D = \sum_{i,j>i} \boldsymbol{u}^*_{ij} \cdot \mathbb{A}_{ij}(r_{ij}) \cdot \boldsymbol{u}^*_{ij}, \tag{7}$$

with a definite positive bilinear form:

$$\mathbb{A}_{ij}(r_{ij}) = F(r_{ij})\,(\zeta_1\, \boldsymbol{e}_{ij} \otimes \boldsymbol{e}_{ij} + \zeta_2\, \boldsymbol{I})\, V_i V_j, \tag{8}$$

in which the coefficients ζ_1, ζ_2 have dimensions of dynamic viscosities.

The introduction of the spin degree of freedom leads to major differences with respect to [16,17], thus justifying the need for the derivations that follow next.

The right-hand side of Eq. (8) is the more general form for a second rank *objective* tensor, constructed from particle coordinates [18]. So defined, and considering the form of the $\boldsymbol{u}^*_{ij}$, this dissipation function is as general as it can be in regards to being invariant to translations and rigid rotations, a property which is crucial in numerical methods for inducing no spurious dissipation. These imposed symmetries in the dissipation function are analogous to the symmetries of the Lagrangian. Effectively, if the dissipation function is invariant under translations and solid body rotations, the total momentum as well as the total angular momentum of the system will be unaffected by the dissipative forces derived from the former.

Applied to $\boldsymbol{u}^*_{ij}$, it leads to

$$\Phi_D = \frac{\zeta_1}{2} \sum_{i,j\neq i} F(r_{ij})\,(\boldsymbol{e}_{ij} \cdot \boldsymbol{u}_{ij})^2\, V_i V_j + \frac{\zeta_2}{2} \sum_{i,j\neq i} F(r_{ij})\,(\boldsymbol{u}_{ij} - \overline{\boldsymbol{\Omega}}_{ij} \times \boldsymbol{r}_{ij})^2\, V_i V_j, \tag{9}$$

where the summation takes now each pair twice, a convention which is possible due to the symmetry of the interactions, and that facilitates some of the deductions later on. Since $F(0) = 0$ for common kernels, the restriction $j \neq i$ in the summation in this equation, and in the ones that follow in the rest of the paper, could ultimately be removed.

The second term in Eq. (9) is the new contribution proposed, and represents the friction between two particles due to the velocity difference in the mid point between the particles, induced by the translational velocities and the spin induced ones.

Notice that in Eqs. (5) and (9) we have made the distinction between the independent variables in the Lagrangian $\dot{\boldsymbol{r}}_i, \boldsymbol{r}_i$, $\dot{\boldsymbol{\theta}}_i$, $\boldsymbol{\theta}_i$ and the ones in the Rayleighian $\boldsymbol{u}_i$, $\boldsymbol{\Omega}_i$, although one assumes that $\dot{\boldsymbol{r}}_i = \boldsymbol{u}_i$ and $\dot{\boldsymbol{\theta}}_i = \boldsymbol{\Omega}_i$, at the end. Moreover, the dissipation function must be a quadratic function of the velocities. Under these conditions, the dynamics of the system is given by

$$\begin{aligned} \frac{d}{dt}\left(\frac{\partial \mathcal{L}}{\partial \dot{\boldsymbol{r}}_i}\right) - \frac{\partial \mathcal{L}}{\partial \boldsymbol{r}_i} &= \mathcal{Q}^V_i\,, \\ \frac{d}{dt}\left(\frac{\partial \mathcal{L}}{\partial \dot{\boldsymbol{\theta}}_i}\right) - \frac{\partial \mathcal{L}}{\partial \boldsymbol{\theta}_i} &= \mathcal{T}^V_i\,, \end{aligned} \tag{10}$$

where $\mathcal{Q}^V_i$, $\mathcal{T}^V_i$ are, respectively, the generalized dissipative forces and torques acting among the particles, which are obtained from differentiation of Φ_D with respect to $\boldsymbol{u}_i$ and $\boldsymbol{\Omega}_i$,

respectively, i.e.,

$$\begin{aligned} \mathcal{Q}_i^V &= -\frac{\partial}{\partial \boldsymbol{u}_i}\Phi_D = -\zeta_1 \sum_j F(r_{ij})(\boldsymbol{u}_{ij}\cdot\boldsymbol{e}_{ij})\boldsymbol{e}_{ij}V_iV_j \\ &\quad - \zeta_2 \sum_j F(r_{ij})(\boldsymbol{u}_{ij} - \overline{\boldsymbol{\Omega}}_{ij}\times\boldsymbol{r}_{ij})V_iV_j, \end{aligned} \tag{11}$$

$$\mathcal{T}_i^V = -\frac{\partial}{\partial \boldsymbol{\Omega}_i}\Phi_D = \frac{\zeta_2}{2}\sum_j F(r_{ij})\boldsymbol{r}_{ij}\times(\boldsymbol{u}_{ij} - \overline{\boldsymbol{\Omega}}_{ij}\times\boldsymbol{r}_{ij})V_iV_j. \tag{12}$$

Equation (11) can be written as

$$\begin{aligned} \mathcal{Q}_i^V &= -\frac{\partial}{\partial \boldsymbol{u}_i}\Phi_D = -\zeta_1 \sum_j F(r_{ij})(\boldsymbol{u}_{ij}\cdot\boldsymbol{e}_{ij})\boldsymbol{e}_{ij}V_iV_j \\ &\quad - \zeta_2 \sum_j F(r_{ij})\boldsymbol{u}_{ij}V_iV_j \\ &\quad + \zeta_2 \sum_j F(r_{ij})(\overline{\boldsymbol{\Omega}}_{ij}\times\boldsymbol{r}_{ij})V_iV_j. \end{aligned} \tag{13}$$

With this notation, as discussed in Ref. [16], the first contribution corresponds to the Monaghan and Gingold's viscous term [19], and the second to the Morris *et al.* viscous term [33]. However, the first term conserves angular momentum while the second does not. As will be seen later in the paper, the third term, the contribution due to the spin and the related spin derivative equation, will allow to correct this matter.

The equation of motion for the rototranslational dynamics of the ensemble of particles obtained from Eq. (10) reads

$$\begin{aligned} m_i\frac{d\boldsymbol{u}_i}{dt} &= m_i\boldsymbol{f}_i^C + m_i\boldsymbol{g}_i + m_i\boldsymbol{f}_i^V, \quad m_i\boldsymbol{f}_i^V := \mathcal{Q}_i^V, \\ m_i\boldsymbol{I}_i\frac{d\boldsymbol{\Omega}_i}{dt} &= m_i\boldsymbol{t}_i^C + m_i\boldsymbol{G}_i + m_i\boldsymbol{t}_i^V, \quad m_i\boldsymbol{t}_i^V := \mathcal{T}_i^V, \end{aligned} \tag{14}$$

where $m_i\boldsymbol{f}_i^C$ is the interparticle conservative force, $\boldsymbol{g}_i$ the acceleration due to the conservative body forces, i.e., $\boldsymbol{g}_i = -\partial U/\partial\boldsymbol{r}_i$, and $\boldsymbol{f}_i^V$ are particle accelerations due to the considered dissipative forces. The second equation of Eqs. (14) governs the particle spin dynamics. In analogy with the first equation, the terms on the right-hand side are: $m_i\boldsymbol{t}_i^C$, the interparticle conservative torque, $\boldsymbol{G}_i$, the angular acceleration due to the body torque field linked to the potential $\mathcal{V}$, i.e., $\boldsymbol{G}_i = -\partial\mathcal{V}/\partial\boldsymbol{\theta}_i$ and finally $\boldsymbol{t}_i^V$ is torque per unit of particle mass due to the considered dissipative torques.

Making use of the properties of internal energy e and translational invariance, one can write $m_i\boldsymbol{f}_i^c$ in Eqs. (14) (see Ref. [16] for details) as

$$\begin{aligned} m_i\boldsymbol{f}_i^C &\equiv -\sum_j m_j\frac{\partial e_j}{\partial \boldsymbol{r}_i} = -\sum_j m_j\frac{\partial e_j}{\partial\rho_j}\bigg|_s\frac{\partial\rho_j}{\partial\boldsymbol{r}_i} \\ &= \sum_j\left[\frac{p_jV_j^2 + p_iV_i^2}{V_iV_j}\right]\boldsymbol{r}_{ij}F(r_{ij})V_iV_j, \end{aligned} \tag{15}$$

where we have used the fact that the particle pressure is linked to the internal energy: $p = \rho^2\partial e/\partial\rho|_s$. In this derivation we have considered that the entropy s is intrinsically carried by the particles and is not a function of the environment, as the local mass density ρ is. Considering that the density field is affected by the particle positions and not by the spatial rotations, in the present model $\boldsymbol{t}_i^C$ is assumed equal to zero.

Equations (14) are integrated in time to describe the dynamics of the system, including the formulated dissipative forces and torques.

B. Conservation of angular momentum

As discussed after introducing Eq. (13), the terms in Eq. (9) lead to two distinct contributions to the viscous force considered. The first one is the Monaghan and Gingold's force:

$$m_i\boldsymbol{f}_i^{\mathrm{MG}} = -\zeta_1\sum_j F(r_{ij})(\boldsymbol{u}_{ij}\cdot\boldsymbol{e}_{ij})\boldsymbol{e}_{ij}V_iV_j. \tag{16}$$

The second contribution is the Morris *et al.* [33] one, but applied to the spin corrected velocity difference Eq. (6):

$$m_i\boldsymbol{f}_i^{\Omega} = -\zeta_2\sum_j F(r_{ij})(\boldsymbol{u}_{ij} - \overline{\boldsymbol{\Omega}}_{ij}\times\boldsymbol{r}_{ij})V_iV_j, \tag{17}$$

This contribution results from the mutual influence between the spin dynamics and the particle translational motion.

According to Eqs. (16) and (17), by permuting the indices we arrive to the conclusion that the contribution of particle j to the force applied to particle i, $m_i\boldsymbol{f}_{ij}^v$, and viceversa, verify

$$m_i\boldsymbol{f}_{ij}^v = -m_j\boldsymbol{f}_{ji}^v. \tag{18}$$

Thus, the total force on the center of mass of the pair is zero and, therefore, the total linear momentum of the system will be a conserved quantity under the action of this force.

Conversely, the torque induced by this force over the pair is not zero, indeed:

$$\begin{aligned} &\boldsymbol{r}_i\times m_i\boldsymbol{f}_{ij}^v + \boldsymbol{r}_j\times m_j\boldsymbol{f}_{ji}^v = \boldsymbol{r}_{ij}\times m_i\boldsymbol{f}_{ij}^v \\ &\quad = \boldsymbol{r}_{ij}\times m_i\left(\boldsymbol{f}_{ij}^{\mathrm{MG}} + \boldsymbol{f}_{ij}^{\Omega}\right) = \boldsymbol{r}_{ij}\times m_i\boldsymbol{f}_{ij}^{\Omega} \neq 0, \end{aligned} \tag{19}$$

which indicates that the forces involved induce a net change in angular momentum. However, it can be easily checked that the torque contributions $(m_i\boldsymbol{t}_{ij}^v + m_j\boldsymbol{t}_{ji}^v)$ in Eq. (14) cancel those in Eq. (19), thus implying that angular momentum is globally conserved.

C. Entropy production

Some energy considerations are necessary to compute the dissipation rate of the model as well as to set reasonable limits to the model's parameters ζ_1, ζ_2.

The total energy of the system of particles is defined through the following contributions:

$$\begin{aligned} \mathcal{E} = \sum_i\Big[&\frac{1}{2}\left(m_i\boldsymbol{u}_i^2 + m_iI_i\boldsymbol{\Omega}_i^2\right) + m_iU(t,\boldsymbol{r}_i) \\ &+ m_i\mathcal{V}(t,\boldsymbol{\theta}_i) + m_ie(\rho_i,s_i)\Big]. \end{aligned} \tag{20}$$

Assuming the system is isolated, differentiating Eq. (20) with respect to the time and considering the conservation of $\mathcal{E}$ we

get

$$\dot{\mathcal{E}} = \sum_i \left[m_i \boldsymbol{u}_i \cdot \frac{d\boldsymbol{u}_i}{dt} + m_i I_i \boldsymbol{\Omega}_i \cdot \frac{d\boldsymbol{\Omega}_i}{dt} - m_i \boldsymbol{u}_i \cdot \boldsymbol{g}_i - m_i \boldsymbol{\Omega}_i \cdot \boldsymbol{G}_i + m_i \frac{de_i}{dt} \right] = 0. \tag{21}$$

As discussed when deducing Eq. (15):

$$p_i = \rho_i^2 \left. \frac{\partial e_i}{\partial \rho_i} \right|_s. \tag{22}$$

In addition, in accordance with the second law, the temperature T_i of a particle is obtained as the variation of the specific internal energy as a consequence of variations of the entropy field:

$$T_i = \left. \frac{\partial e_i}{\partial s_i} \right|_V. \tag{23}$$

Considering this and the continuity equation,

$$\frac{d\rho_i}{dt} = \sum_j \left[\frac{\partial \rho_i}{\partial \boldsymbol{r}_j} \cdot \boldsymbol{u}_j \right], \tag{24}$$

the time derivative of the internal energy can be expressed as

$$\frac{de_i}{dt} = \left. \frac{\partial e_i}{\partial \rho_i} \right|_s \frac{d\rho_i}{dt} + \left. \frac{\partial e_i}{\partial s_i} \right|_V \frac{ds_i}{dt} = \frac{p_i}{\rho_i^2} \sum_j \left[\frac{\partial \rho_i}{\partial \boldsymbol{r}_j} \cdot \boldsymbol{u}_j \right] + T_i \frac{ds_i}{dt}. \tag{25}$$

Multiplying the first equation of Eqs. (14) by $\boldsymbol{u}_i$ and the second equation by $\boldsymbol{\Omega}_i$, substituting both and de_i/dt in Eq. (21), one finally gets

$$\sum_i \left[m_i \boldsymbol{f}_i^v \cdot \boldsymbol{u}_i + m_i \boldsymbol{t}_i^v \cdot \boldsymbol{\Omega}_i + m_i T_i \frac{ds_i}{dt} \right] = 0. \tag{26}$$

If the forces and torques in Eq. (26) are dissipative, then by the Second Law of Thermodynamics the entropy production of the system must be positive, i.e.,

$$\sum_i \left[m_i T_i \frac{ds_i}{dt} \right] = -\sum_i \left[m_i \boldsymbol{f}_i^v \cdot \boldsymbol{u}_i + m_i \boldsymbol{t}_i^v \cdot \boldsymbol{\Omega}_i \right] \geqslant 0. \tag{27}$$

If the right-hand side is expanded in its various terms, one gets

$$\begin{aligned} -\sum_i \left[m_i \boldsymbol{f}_i^v \cdot \boldsymbol{u}_i + m_i \boldsymbol{t}_i^v \cdot \boldsymbol{\Omega}_i \right] &= \sum_i \Bigg[\zeta_1 \boldsymbol{u}_i \cdot \sum_j F(r_{ij})(\boldsymbol{u}_{ij} \cdot \boldsymbol{e}_{ij}) \boldsymbol{e}_{ij} V_i V_j \\ &+ \zeta_2 \boldsymbol{u}_i \cdot \sum_j F(r_{ij})(\boldsymbol{u}_{ij} - \overline{\boldsymbol{\Omega}}_{ij} \times \boldsymbol{r}_{ij}) V_i V_j \\ &- \frac{\zeta_2}{2} \boldsymbol{\Omega}_i \cdot \sum_j F(r_{ij}) \boldsymbol{r}_{ij} \times (\boldsymbol{u}_{ij} - \overline{\boldsymbol{\Omega}}_{ij} \times \boldsymbol{r}_{ij}) V_i V_j \Bigg]. \end{aligned} \tag{28}$$

It can be seen (see Appendix A) that the right-hand side of Eq. (28) is equal to dissipation function Φ_d. Therefore, Eq. (27) implies that

$$\Phi_D \geqslant 0. \tag{29}$$

From the entropy production we can derive important conclusions about the restrictions on the values of the dissipative coefficients in the present model. To do so, let us rewrite the right-hand side of Eq. (28) as

$$\Phi_D = \frac{1}{2} \sum_{i,j} V_i V_j F_{ij} [\zeta_1 (\boldsymbol{u}_{ij} \cdot \boldsymbol{e}_{ij})^2 + \zeta_2 (\boldsymbol{u}_{ij} - \overline{\boldsymbol{\Omega}}_{ij} \times \boldsymbol{r}_{ij})^2] \tag{30}$$

and introduce the unit vector $\boldsymbol{\tau}_{ij}$ normal to $\boldsymbol{e}_{ij}$, such that the velocity field $\boldsymbol{u}_{ij}$ is decomposed as follows:

$$\boldsymbol{u}_{ij} = (\boldsymbol{u}_{ij} \cdot \boldsymbol{e}_{ij}) \boldsymbol{e}_{ij} + (\boldsymbol{u}_{ij} \cdot \boldsymbol{\tau}_{ij}) \boldsymbol{\tau}_{ij}. \tag{31}$$

Substituting the expression above inside the formula for Φ_D we find

$$\Phi_D = \frac{1}{2} \sum_{i,j} V_i V_j F_{ij} \{\zeta_1 (\boldsymbol{u}_{ij} \cdot \boldsymbol{e}_{ij})^2 + \zeta_2 [(\boldsymbol{u}_{ij} \cdot \boldsymbol{e}_{ij}) \boldsymbol{e}_{ij} - \boldsymbol{h}_{ij}]^2 \},$$

where

$$\boldsymbol{h}_{ij} := (\boldsymbol{u}_{ij} \cdot \boldsymbol{\tau}_{ij}) \boldsymbol{\tau}_{ij} - \overline{\boldsymbol{\Omega}}_{ij} \times \boldsymbol{r}_{ij}. \tag{32}$$

We observe that $\boldsymbol{h}_{ij} \cdot \boldsymbol{e}_{ij} = 0$, since $\boldsymbol{e}_{ij}$ is parallel to $\boldsymbol{r}_{ij}$ and $\boldsymbol{\tau}_{ij} \cdot \boldsymbol{e}_{ij} = 0$ by definition. Then, expanding the second term inside the summation and rearranging, we find

$$\Phi_D = \frac{1}{2} \sum_{i,j} V_i V_j F_{ij} [(\zeta_1 + \zeta_2)(\boldsymbol{u}_{ij} \cdot \boldsymbol{e}_{ij})^2 + \zeta_2 \|\boldsymbol{h}_{ij}\|^2].$$

To guarantee the positiveness of Φ_D, it is sufficient to require

$$\zeta_2 \geqslant 0 \quad \text{and} \quad \zeta_1 \geqslant -\zeta_2. \tag{33}$$

III. FROM THE DISCRETE TO THE CONTINUUM

A. Momentum equation

As demonstrated by the authors in Ref. [16], the continuous equivalent of the integral form (the limit in which the volume of each particle goes to zero) of the force $\boldsymbol{f}^{\mathrm{MG}}$, Eq. (16), is written in the continuum as a force per unit volume $\rho \boldsymbol{f}^{\mathrm{MG}}$:

$$\rho \boldsymbol{f}^{\mathrm{MG}}(\boldsymbol{r}) = \frac{\zeta_1}{2(n+2)} \nabla^2 \boldsymbol{u}(\boldsymbol{r}) + \frac{\zeta_1}{n+2} \nabla (\nabla \cdot \boldsymbol{u})(\boldsymbol{r}) + O(h^2), \tag{34}$$

where n is the spatial dimensionality of the problem.

As for the other contribution to the dissipative force, $\boldsymbol{f}^{\Omega}$, Eq. (17), let us split it in two parts:

$$\rho_i \boldsymbol{f}_i^{\Omega'} = -\zeta_2 \sum_j F(r_{ij}) \boldsymbol{u}_{ij} V_j, \tag{35}$$

$$\rho_i \boldsymbol{f}_i^{\Omega''} = \zeta_2 \sum_j F(r_{ij}) (\overline{\boldsymbol{\Omega}}_{ij} \times \boldsymbol{r}_{ij}) V_j. \tag{36}$$

Regarding $\boldsymbol{f}_i^{\Omega'}$, also in Ref. [16] it is shown that the continuous equivalent of Eq. (35) is

$$\rho \boldsymbol{f}^{\Omega'}(\boldsymbol{r}) = \frac{\zeta_2}{2} \nabla^2 \boldsymbol{u}(\boldsymbol{r}) + O(h^2). \tag{37}$$

Regarding $\boldsymbol{f}_i^{\Omega\prime\prime}$, using the definition of $\overline{\boldsymbol{\Omega}}_{ij} \times \boldsymbol{r}_{ij}$ in Eq. (6), Eq. (36) can be rewritten as

$$\rho_i \boldsymbol{f}_i^{\Omega\prime\prime} = \frac{\zeta_2}{2}\boldsymbol{\Omega}_i \times \left(\sum_j F(r_{ij})\boldsymbol{r}_{ij}V_j\right) + \frac{\zeta_2}{2}\sum_j F(r_{ij})(\boldsymbol{\Omega}_j \times \boldsymbol{r}_{ij})V_j. \tag{38}$$

The first term is zero in the continuum, as it is an approximation of the integral of the kernel derivative in a system considered isotropic, while the second one is a discretization of $\nabla \times \boldsymbol{\Omega}$ (see, e.g., Ref. [47]). Both are of order h^2 in their integral form. Therefore,

$$\rho \boldsymbol{f}^{\Omega}(\boldsymbol{r}) = \frac{\zeta_2}{2}\nabla^2\boldsymbol{u}(\boldsymbol{r}) + \frac{\zeta_2}{2}\nabla \times \boldsymbol{\Omega} + O(h^2). \tag{39}$$

Collecting back the terms together and taking the limit when the smoothing length, h, goes to zero, one gets

$$\rho \boldsymbol{f}^{v}(\boldsymbol{r}) = \left(\frac{\zeta_1}{2(n+2)} + \frac{\zeta_2}{2}\right)\nabla^2\boldsymbol{u}(\boldsymbol{r}) + \frac{\zeta_1}{n+2}\nabla\,(\nabla \cdot \boldsymbol{u})(\boldsymbol{r}) + \frac{\zeta_2}{2}\nabla \times \boldsymbol{\Omega}. \tag{40}$$

The viscous force in Eq. (40) has the structure of the Newtonian one plus a rotational term. Together with the pressure term and the body force, they lead to the continuous momentum equation:

$$\rho\frac{d\boldsymbol{u}}{dt} = -\nabla p + \rho \boldsymbol{f}^{v} + \rho \boldsymbol{g}. \tag{41}$$

It is germane to mention that Müller *et al.* [31] proposed, for their model, this same dissipative term Eq. (40) with, however, three degrees of freedom: a shear, a second, and a rotational viscosity, postulating *a posteriori* restrictions in their values. In present paper, it has been shown that by deriving this force with a bottom-up approach from the particle level, only two coefficients are actually necessary to set the intensity of the dissipation mechanisms involved due to the restrictions imposed by the required symmetry of the dissipation function in Eq. (9).

B. Spin equation

Let us recall the second Eq. in (14), making explicit its right-hand side:

$$m_i I_i \frac{d\boldsymbol{\Omega}_i}{dt} = m_i \boldsymbol{G}_i + \frac{\zeta_2}{2}\sum_j F(r_{ij})\boldsymbol{r}_{ij} \times (\boldsymbol{u}_{ij} - \overline{\boldsymbol{\Omega}}_{ij} \times \boldsymbol{r}_{ij})V_i V_j. \tag{42}$$

To move to the continuum, let us divide Eq. (42) by the particle volume V_i and split the second term in the right-hand side in Eq. (42) in its two summands:

$$\rho_i I_i \frac{d\boldsymbol{\Omega}_i}{dt} = \rho_i \boldsymbol{G}_i + \frac{\zeta_2}{2}\left[\sum_j F(r_{ij})(\boldsymbol{r}_{ij} \times \boldsymbol{u}_{ij})V_j - \sum_j F(r_{ij})\boldsymbol{r}_{ij} \times (\overline{\boldsymbol{\Omega}}_{ij} \times \boldsymbol{r}_{ij})V_j\right]. \tag{43}$$

The first term is a second order approximation to $\nabla \times \boldsymbol{u}$ (see, e.g., Ref. [47]) in the integral form, while for the second term (see Appendix B):

$$\sum_j F(r_{ij})\boldsymbol{r}_{ij} \times (\overline{\boldsymbol{\Omega}}_{ij} \times \boldsymbol{r}_{ij})V_j = 2\boldsymbol{\Omega}_i + O(h^2). \tag{44}$$

Combining both, and taking the limit when the smoothing length, h, goes to zero, one gets the continuum analog of Eq. (42),

$$\rho \mathcal{I}\frac{d\boldsymbol{\Omega}}{dt} = \rho \boldsymbol{G} - \frac{\zeta_2}{2}(2\boldsymbol{\Omega} - \nabla \times \boldsymbol{u}). \tag{45}$$

In Appendix C a discussion on the physical meaning of the moment of inertia per unit of mass $\mathcal{I}$ is provided. A proposal for assigning it a specific value in the numerical simulations is also there included.

C. Identification of the present model with a continuous micropolar model

The micropolar viscous force per unit volume in the momentum equation has the form (see Ref. [20], chap. 3):

$$\rho \boldsymbol{f}^{\mathrm{mp}} = (\mu + \mu_r)\nabla^2\boldsymbol{u} + (\mu + \lambda - \mu_r)\nabla\,(\nabla \cdot \boldsymbol{u}) + 2\mu_r \nabla \times \boldsymbol{\Omega}, \tag{46}$$

where μ, λ and μ_r are the shear, second and microrotation viscosities, respectively.

Comparing Eq. (46) with the force derived in present work [Eq. (40)] one gets the following dependence of these parameters with the two independent coefficients of present model ζ_1, ζ_2:

$$\begin{aligned} \mu &= \frac{\zeta_1}{2(n+2)} + \frac{\zeta_2}{4}, \\ \lambda &= \frac{\zeta_1}{2(n+2)}, \Rightarrow \mu_r = \mu - \lambda, \\ \mu_r &= \frac{\zeta_2}{4}. \end{aligned} \tag{47}$$

Since, as shown in Sec. II C, $\zeta_1 \geqslant -\zeta_2$, $\zeta_2 \geqslant 0$, the following limits apply to μ, μ_r, and λ:

$$\begin{aligned} &\mu \geqslant 0, \\ &\mu_r \geqslant 0, \\ &-\frac{2\mu}{n} \leqslant \lambda \leqslant \mu, \Rightarrow 0 \leqslant \mu_r \leqslant \mu\left(1 + \frac{2}{n}\right). \end{aligned} \tag{48}$$

As for the bulk viscosity κ_B, defined as (see Ref. [48]):

$$\kappa_B = \lambda + \frac{2\mu}{n}, \tag{49}$$

the following limits apply for κ_B in the micropolar fluid model developed herein, as a consequence of those of μ and λ:

$$0 \leqslant \kappa_B \leqslant \mu\left(1 + \frac{2}{n}\right). \tag{50}$$

The lower limit, $\kappa_B = 0$, corresponds to fluids which verify the Stokes' hypothesis. Contrary to the standard SPH viscous

terms, which, as shown in our previous work [16], do not allow to model such fluids, the proposed model certainly allows to reach that lower limit for the bulk viscosity.

Regarding the upper limit, it implies that with the present fluid model, if a large bulk viscosity is necessary, then a large shear viscosity, μ, will have to be considered too. Summarizing, the bulk and shear viscosity are independent, but the range of admissible bulk viscosities is a function of the shear one. To overcome this limitation, the bulk viscosity model and associated dissipation function, developed by the authors [17], should be added to the present model, which is an alternative that presents no additional difficulty, and remains in the same theoretical framework.

It is interesting to point out at this stage that if Eq. (46) is reshaped using that

$$\nabla^2 \boldsymbol{u} = \boldsymbol{\nabla}\,(\boldsymbol{\nabla}\cdot\boldsymbol{u}) - \boldsymbol{\nabla}\times(\boldsymbol{\nabla}\times\boldsymbol{u}), \tag{51}$$

one gets

$$\rho \boldsymbol{f}^{\mathrm{mp}} = \mu\,\nabla^2\boldsymbol{u} + (\mu+\lambda)\boldsymbol{\nabla}\,(\boldsymbol{\nabla}\cdot\boldsymbol{u}) + \mu_r\boldsymbol{\nabla} \times (2\boldsymbol{\Omega} - \boldsymbol{\nabla}\times\boldsymbol{u}). \tag{52}$$

If the spin is equal to half the vorticity, then Eq. (52) becomes the standard Navier-Stokes momentum equation for Newtonian fluids. Indeed, as discussed in Sec. II C, by inspecting the spin evolution equation, Eq. (45), one can see that, in the present model, the spin is equal to half the vorticity if the inertial term on its left-hand side is zero, provided the external body torque is zero. Under these conditions, the model developed so far reduces to that of a Newtonian fluid.

Also, under these conditions, the momentum Eq. (52) gets decoupled from the spin evolution one, Eq. (45). A general isotropic micropolar fluid model, in which the dissipation function is enriched with terms depending on the spatial derivatives of the spin, can be developed. For this model, the referred uncoupling does not occur. This general isotropic micropolar fluid model will be obtained and validated next.

It is important to note that the momentum equation for micropolar viscous flows (46) adopted in this section is the one proposed by Condiff and Dahler [21] and later used by Lukaszewicz in his book [20]. However, authors like Eringen [22] proposed alternative constitutive laws by redefining the viscosity coefficients. Indeed, in Ref. [22] the following equation, equivalent to Eq. (46), was proposed:

$$\rho \boldsymbol{f}^{\mathrm{mp}} = (\mu+\kappa)\,\nabla^2\boldsymbol{u} + (\mu+\lambda)\boldsymbol{\nabla}\,(\boldsymbol{\nabla}\cdot\boldsymbol{u}) + \kappa\boldsymbol{\nabla}\times\boldsymbol{\Omega}, \tag{53}$$

with the corresponding, also equivalent, spin equation:

$$\rho\mathcal{I}\frac{d\boldsymbol{\Omega}}{dt} = \rho\boldsymbol{G} - \kappa(2\boldsymbol{\Omega} - \boldsymbol{\nabla}\times\boldsymbol{u}). \tag{54}$$

In this latter formulation the rotational viscosity is referred to as κ. When this alternative formulation is used, the dependence of its coefficients (μ, κ, λ) with ζ_1 and ζ_2 needs to be consistently readjusted, changing Eqs. (47) accordingly. This Eringen's [22] alternative formulation is used in one of the reference solutions considered in Sec. V.

IV. A GENERAL ISOTROPIC MICROPOLAR FLUID MODEL IN SPH

Inspired by Condiff and Dahler [21], the following dissipation function Φ'_D is now proposed, extending Φ_D defined in Eq. (7) to account for dissipation mechanisms based on spin derivatives:

$$\Phi'_D = \Phi_D + \Phi^{\Omega}_D, \tag{55}$$

with

$$\Phi^{\Omega}_D = \sum_{i,j>i} \boldsymbol{\Omega}_{ij}\cdot\ \mathbb{B}_{ij}(r_{ij})\ \cdot\boldsymbol{\Omega}_{ij}, \tag{56}$$

where $\boldsymbol{\Omega}_{ij} := \boldsymbol{\Omega}_i - \boldsymbol{\Omega}_j$, and where $\mathbb{B}$ is an objective tensor of second rank, with the same structure like $\mathbb{A}$, as defined in Eq. (8):

$$\mathbb{B}_{ij}(r_{ij}) = F(r_{ij})(\xi_1\boldsymbol{e}_{ij}\otimes\boldsymbol{e}_{ij} + \xi_2\boldsymbol{I})V_iV_j. \tag{57}$$

This is the most general form that preserves translational and solid-body rotational invariance of the dissipation function in Eq. (56). It is noted that the dimensions of the viscosity coefficients ζ_1, ζ_2 and ξ_1, ξ_2 are different.

From Eqs. (56) and (57), the following expression for Φ^{Ω}_D is obtained:

$$\Phi^{\Omega}_D = \frac{\xi_1}{2}\sum_{i,j\neq i} F(r_{ij})(\boldsymbol{e}_{ij}\cdot\boldsymbol{\Omega}_{ij})^2V_iV_j + \frac{\xi_2}{2}\sum_{i,j\neq i} F(r_{ij})\boldsymbol{\Omega}^2_{ij}V_iV_j. \tag{58}$$

Since Φ^{Ω}_D depends only on the spin derivatives, it impacts only on the viscous torque $m_i\boldsymbol{t}^v_i$, as computed with Eq. (14), redefined now as

$$\begin{aligned} m_i\boldsymbol{t}^v_i &= -\frac{\partial}{\partial\boldsymbol{\Omega}_i}\Phi_D - \frac{\partial}{\partial\boldsymbol{\Omega}_i}\Phi^{\Omega}_D \\ &= \frac{\zeta_2}{2}\sum_j F(r_{ij})\boldsymbol{r}_{ij}\times(\boldsymbol{u}_{ij} - \overline{\boldsymbol{\Omega}}_{ij}\times\boldsymbol{r}_{ij})V_iV_j \\ &\quad - \xi_1\sum_j F(r_{ij})(\boldsymbol{e}_{ij}\cdot\boldsymbol{\Omega}_{ij})\boldsymbol{e}_{ij}V_iV_j - \xi_2\sum_i F(r_{ij})\boldsymbol{\Omega}_{ij}V_iV_j. \end{aligned} \tag{59}$$

This viscous torque modifies the right-hand side in Eq. (14) to get a general micropolar model. The first term in Eq. (59) comes from Φ_D and was already presented in Eq. (12). The second and the third derive from Φ^{Ω}_D.

It is important to highlight that the two additional terms on ξ_1 and ξ_2 in Eq. (59) are antisymmetric for two generic particles i and j. Therefore, they do not change the angular momentum of the system, thus keeping the property of the whole scheme of being angular momentum conservative.

To take the torque in Eq. (59) back to the continuum, the same principles of Sec. III A are used, to which the result for the torque in Sec. III B is added, leading to a modified equation for the spin evolution at the continuous level:

$$\rho\mathcal{I}\frac{d\boldsymbol{\Omega}}{dt} = \rho\boldsymbol{G} - 2\mu_r(2\boldsymbol{\Omega} - \boldsymbol{\nabla}\times\boldsymbol{u}) + \gamma_1\nabla^2\boldsymbol{\Omega} + (\gamma_1+\gamma_2)\boldsymbol{\nabla}\,(\boldsymbol{\nabla}\cdot\boldsymbol{\Omega}), \tag{60}$$

where the additional spin-viscosity coefficients γ_1 and γ_2 are linked to the parameters ξ_1 and ξ_2 through

$$\gamma_1 = \left[\frac{\xi_1}{2(n+2)} + \frac{\xi_2}{2}\right], \quad \gamma_2 = \left[\frac{\xi_1}{2(n+2)} - \frac{\xi_2}{2}\right], \tag{61}$$

and where we have implicitly assumed that $n \geqslant 3$. For $n = 2$, namely, in the case that two-dimensional simulations are performed (not to be confused with two dimensional flows studied through three-dimensional simulations), vorticity and spin are transported as scalars. Then, in Eq. (59), the term proportional to ξ_1 is exactly zero and should be ignored. In terms of viscosity coefficients, this implies that $\gamma_2 = -\gamma_1$. Hence, the transport coefficients given in Eq. (61), for two dimensions correspond to the ones of Eq. (59) with $\xi_1 = 0$. In what follows, ξ_1 should be set equal to zero or ignored if two-dimensional simulations are to be considered.

The evolution equation for the spin derivative Eq. (60) includes the same additional terms (spin Laplacian and gradient of spin divergence) like the corresponding one in the referred seminal paper by Condiff and Dahler [21] [Eq. (13) there].

The entropy production is increased by these additional terms (the procedure is similar to the one followed in Sec. II C), with analogous restrictions for ξ_1 and ξ_2 as the ones for ζ_1 and ζ_2, expressed in Eq. (33). Therefore, $\xi_2 \geqslant 0$ and $\xi_1 \geqslant -\xi_2$. It is worth noting that for planar flows $(\boldsymbol{\nabla} \cdot \boldsymbol{\Omega})$ is zero.

An important conclusion of this general model, as given in Eq. (60), is that the micropolar effects can exist even if the rotational inertia of the system is negligible in the continuum description provided an external body torque is absent. Effectively, for a fluid of small physical particles with no relevant moment of inertia, $\mathcal{I}$ is vanishingly small. However, when equating the left-hand side of Eq. (60) to zero, due to the presence of the new dissipative terms still the spin field $\boldsymbol{\Omega}$ is not equal to the vorticity but satisfies a spatial differential equation. It is thus expected that this general micropolar model can find application to the modeling of non-Newtonian fluids, in which the microscopic structure of the molecules can introduce this type of dissipative processes given in Eq. (58). The general micropolar isotropic model proposed in this section will be the one used in the verification and validation cases that follow next.

V. NUMERICAL VERIFICATION AND VALIDATION

A. SPH scheme for micropolar fluid

The SPH equations described in the previous sections are implemented numerically and validated against analytical and numerical solutions available in the literature. For the sake of clearness, the final SPH equations read

$$\begin{aligned}\rho_i \frac{d\boldsymbol{u}_i}{dt} = &-\sum_j \left[\frac{p_j V_j^2 + p_i V_i^2}{V_i V_j}\right] \boldsymbol{r}_{ij} F(r_{ij}) V_j + \rho_i \boldsymbol{g}_i \\ &- (\mu - \mu_r) 2(n+2) \sum_j F(r_{ij}) (\boldsymbol{u}_{ij} \cdot \boldsymbol{e}_{ij}) \boldsymbol{e}_{ij} V_j \\ &- 4\mu_r \sum_j F(r_{ij}) (\boldsymbol{u}_{ij} - \overline{\boldsymbol{\Omega}}_{ij} \times \boldsymbol{r}_{ij}) V_j\end{aligned}$$

$$\begin{aligned}\rho_i I_i \frac{d\boldsymbol{\Omega}_i}{dt} = &\rho_i \boldsymbol{G}_i + 2\mu_r \sum_j F(r_{ij}) \boldsymbol{r}_{ij} \times (\boldsymbol{u}_{ij} - \overline{\boldsymbol{\Omega}}_{ij} \times \boldsymbol{r}_{ij}) V_j \\ &- (\gamma_1 + \gamma_2)(n+2) \sum_j F(r_{ij}) (\boldsymbol{e}_{ij} \cdot \boldsymbol{\Omega}_{ij}) \boldsymbol{e}_{ij} V_j \\ &- (\gamma_1 - \gamma_2) \sum_i F(r_{ij}) \boldsymbol{\Omega}_{ij} V_j.\end{aligned} \tag{62}$$

These correspond to the following continuous equations:

$$\begin{aligned}\rho \frac{d\boldsymbol{u}}{dt} = &-\boldsymbol{\nabla} p + \rho \boldsymbol{g} + \mu \nabla^2 \boldsymbol{u} + (\mu + \lambda) \boldsymbol{\nabla} (\boldsymbol{\nabla} \cdot \boldsymbol{u}) \\ &+ \mu_r \boldsymbol{\nabla} \times (2\boldsymbol{\Omega} - \boldsymbol{\nabla} \times \boldsymbol{u}), \\ \rho \mathcal{I} \frac{d\boldsymbol{\Omega}}{dt} = &\rho \boldsymbol{G} + \gamma_1 \nabla^2 \boldsymbol{\Omega} + (\gamma_1 + \gamma_2) \boldsymbol{\nabla} (\boldsymbol{\nabla} \cdot \boldsymbol{\Omega}) \\ &- 2\mu_r (2\boldsymbol{\Omega} - \boldsymbol{\nabla} \times \boldsymbol{u}),\end{aligned} \tag{63}$$

where $\lambda = (\mu - \mu_r)$, as implied by the SPH model (see the discussion in the Sec. III C). Moreover, we recall that an additional constraint, namely, $\gamma_2 = -\gamma_1$, needs to be imposed when the flow is planar (see Sec. IV).

In this latter case, some authors, such as, for example, Venkatadri *et al.* [49], provide the numerical solution of Eq. (63) by using a vorticity-spin formulation. The vorticity equation is obtained by performing the curl of the momentum Eq. (63) and, for an incompressible fluid in a two dimensional framework, the vorticity-spin formulation reads as follows:

$$\begin{aligned}\rho \frac{d\omega}{dt} &= \mu \nabla^2 \omega - \mu_r \nabla^2 (2\Omega - \omega), \\ \rho \mathcal{I} \frac{d\Omega}{dt} &= \gamma_1 \nabla^2 \Omega - 2\mu_r (2\Omega - \omega) + \rho \boldsymbol{G},\end{aligned} \tag{64}$$

where ω is the scalar vorticity field. Incidentally, Venkatadri *et al.* [49] set

$$\gamma_1 = \mu \mathcal{I}, \tag{65}$$

which allows to combine the two equations above in the following compact form:

$$\rho \frac{dS}{dt} = (\mu + \mu_r) \Delta S - \frac{4\mu_r}{\mathcal{I}} S + \frac{2\rho}{\mathcal{I}} \boldsymbol{G}, \tag{66}$$

where $S = 2\Omega - \omega$. In this form, S can be independently evolved in time.

Moreover, as pointed out by Ahmadi [50], if the relationship Eq. (65) holds (and assuming that $\boldsymbol{G} = 0$), then the spin, Ω, would fulfill the vorticity evolution equation in Eq. (64), provided the initial and boundary conditions for both flow fields are the same. However, such an assumption, Eq. (65), is unnecessarily restrictive, preventing the model from covering all the phenomenology it encompasses.

Before proceeding to the description of the test cases, we address some aspects that are important for the numerical implementation. In all the simulations $\mu_r/\mu = O(1)$ is considered and, according to the constraint in the Eq. (48), $\mu_r/\mu = 2$ is selected as limiting case (zero bulk viscosity). The chosen Reynolds numbers, namely, $\mathrm{Re} = \rho U L/\mu$ and $\mathrm{Re}^{\Omega} = \rho U \mathcal{I}/(2\mu_r L)$ where U and L are the reference velocity and length scales, correspond to moderate regimes. For

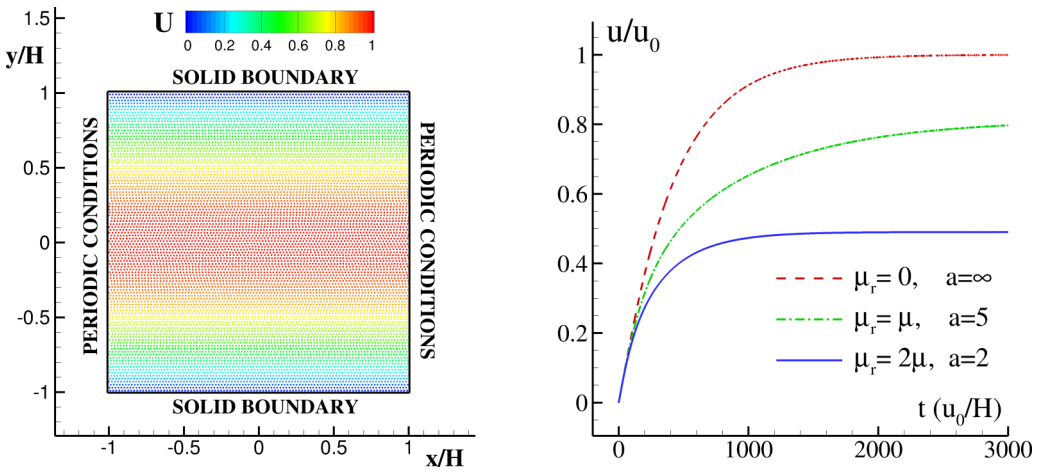

FIG. 2. Micropolar Poiseuille flow. Left: snapshot of the velocity field in the fluid domain ($\mu_r = 0; a = \infty$). Right: time histories of the horizontal velocity recorded at the center of the fluid domain for three cases: ($\mu_r = 0; a = \infty$), ($\mu_r = \mu; a = 5$), and ($\mu_r = 2\mu; a = 2$). The spatial resolution is $N = H/\Delta r = 50$.

confined flows (as for the selected test cases), these regimes represent troublesome simulations for the SPH scheme.

Indeed, the particle spatial disorder generally increases during the time evolution and induces large errors. It has to be borne in mind that in the initial condition the particles are placed in a lattice and that, due the Lagrangian nature of the solver, they are transported by the flow, therefore breaking that initial lattice. Under these conditions, the accuracy of the differential operators degrades [44].

Furthermore, the development of the so-called tensile-instability [51], which leads to nonphysical clustering of particles, may even impede the attainment of an accurate numerical solution. For the above reasons, the δ-ALE-SPH scheme [52] has been adopted for integrating the SPH equations. In this model a Particle Shifting Technique (PST) is used to regularize the particle positions during the time evolution, thus improving the robustness and the accuracy of the numerical scheme.

A Wendland C-2 kernel [53] has been used in all simulations.

B. Poiseiulle flow with a micropolar fluid

In the literature on micropolar fluid flows there are a number of exact solutions that may be used for verification of the generalized numerical scheme developed in present paper. An extensive review is contained in Ariman *et al.* [23] and some of these solutions are discussed in detail by Stokes [18]. In particular, in Chapter 6, steady-state 2D flows between parallel plates in the absence of gravity were presented. Among them we select a Poiseuille flow to be treated from the practical point of view as a periodic flow in x. The flow fields have the following form:

$$\boldsymbol{u} = (u(y), 0), \quad \boldsymbol{\Omega} = \Omega(y). \tag{67}$$

The steady-state form of the motion Eqs. (63) reads

$$-\frac{dp}{dx} + (\mu + \mu_r)\frac{d^2u}{dy^2} + 2\mu_r\frac{d\Omega}{dy} = 0, \tag{68}$$

$$\gamma_1\frac{d^2\Omega}{dy^2} - 2\mu_r\frac{du}{dy} - 4\mu_r\Omega = 0. \tag{69}$$

Let us denote the distance between the plates as $2H$. The boundary conditions read

$$u(\pm H) = 0, \quad \Omega(\pm H) = 0. \tag{70}$$

The general solution of Eqs. (68) and (69) is (see Ref. [18])

$$U(\xi) = \frac{u(\xi)}{u_0} = 1 - \xi^2 - \left(\frac{2\mu_r}{\mu + \mu_r}\right) \times \frac{\cosh a}{a \sinh a}\left[1 - \frac{\cosh(a\xi)}{\cosh a}\right], \tag{71}$$

$$\omega(\xi) = \frac{u_0}{H}\left[2\xi - \left(\frac{2\mu_r}{\mu + \mu_r}\right)\frac{\sinh(a\xi)}{\sinh a}\right], \tag{72}$$

$$\Omega(\xi) = \frac{u_0}{H}\left[\xi - \frac{\sinh(a\xi)}{\sinh a}\right], \tag{73}$$

with

$$\xi = \frac{y}{H}, \quad u_0 = -\frac{H^2}{2\mu}\frac{dp}{dx}, \quad a = \frac{H}{l}, \quad l^2 = \frac{\gamma_1}{4\mu}\left[\frac{1 + \mu_r/\mu}{\mu_r/\mu}\right]. \tag{74}$$

Incidentally, we observe that the analytical solution depends on the choice of two parameters, namely μ/μ_r and a (or, equivalently, γ_1/μ).

The Reynolds number adopted for the numerical simulations is $\mathrm{Re} = \rho u_0 H/\mu = 1000$. The fluid starts from rest conditions and, after a certain transient, reaches a steady state condition. The computational fluid domain is depicted in the left panel of Fig. 2 at the steady state for ($\mu_r = 0; a = \infty$), while the right panel of the same figure shows the velocity profiles recorded at the center of the fluid domain during the transient for three choices of the parameters (μ_r, a). The case ($\mu_r = 0; a = \infty$) corresponds to the classic Poiseuille flow with a parabolic profile for the velocity field. As can be expected, an increase of the viscous parameter μ_r leads to a decrease of the steady-state velocity.

Figure 3 displays the profiles of the velocity, vorticity and spin during the transient and at the steady state for the cases

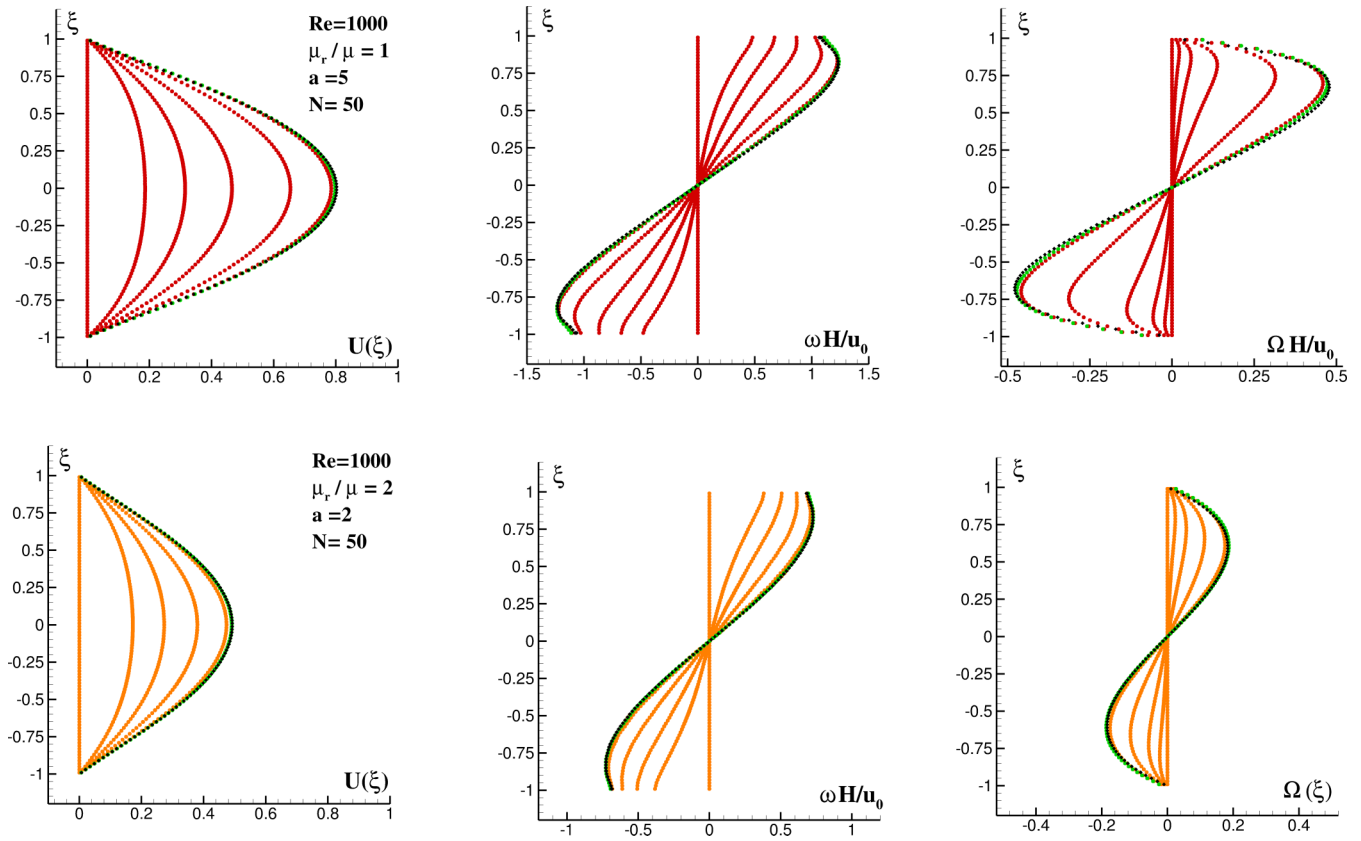

FIG. 3. Micropolar Poiseuille flow: Profiles of the velocity (left), vorticity (middle), and spin (right) during the transient (red/orange dots, time instants $tU/H = 0, 100, 200, 400, 1000, 2500$) and the steady-state (green dots, $tU/H = 3000$) for ($\mu_r/\mu = 1, a = 5$) (top panels) and ($\mu_r/\mu = 2, a = 2$) (bottom panels). Black-diamond dots indicate the analytical solution.

($\mu_r/\mu = 1, a = 5$) (top panels) and ($\mu_r/\mu = 2, a = 2$) (bottom panels). The comparisons with the analytical solution are good in all the cases. In comparison with the classic Poiseuille flow, the velocity profile remains similar to a parabola and only minor changes are observed close to the walls. However, the vorticity deviates significantly from the Newtonian solution linear profile close to the solid boundaries (see the right panel of Fig. 3).

Despite the steady-state numerical solutions are not affected by the value of the micropolar inertia, this plays an important role during the time integration. In all the simulations we adopted $\mathcal{I}/H^2 = 2$ which corresponds to a relaxation time $\tau U/H = \mathrm{Re}^{\Omega} = \rho U \mathcal{I}/(2\mu_r H) = 1000$ for the test case ($\mu_r/\mu = 1$) and $\tau U/H = 500$ for the second test case ($\mu_r/\mu = 2$) (see the Appendix C for details).

Table I shows a convergence analysis for the chosen cases. Specifically, it displays the relative errors for the velocity recorded at the center of the domain:

$$\epsilon_U = \frac{\left|U_C^N - U_C^{\mathrm{ana}}\right|}{U_C^{\mathrm{ana}}}$$

and the relative errors for the kinetic energy on the whole domain:

$$\epsilon_K = \frac{\left|\mathcal{E}_K^N - \mathcal{E}_K^{\mathrm{ana}}\right|}{\mathcal{E}_K^{\mathrm{ana}}}.$$

The spatial resolution is indicated through $N = H/\Delta r$, where Δr is the initial particle distance. Apart from the case with ($\mu_r/\mu = 2, a = 2$), the SPH model predicts a convergence rate between 1 and 2, in agreement with the usual convergence

TABLE I. Micropolar Poiseuille flow: Convergence toward the analytical solution for the three test-cases simulated. Here ϵ_U is the relative error on velocity recorded at the center of the fluid domain and ϵ_K is the relative error on the global kinetic energy. The spatial resolution is $N = H/\Delta r$, where Δr is the initial particle distance.

$\mu_r = 0; a = \infty$			$\mu_r = \mu; a = 5$			$\mu_r = 2\mu; a = 2$		
N	$\epsilon_U(\%)$	$\epsilon_K(\%)$	N	$\epsilon_U(\%)$	$\epsilon_K(\%)$	N	$\epsilon_U(\%)$	$\epsilon_K(\%)$
25	0.21	0.52	25	1.28	2.60	25	0.41	0.54
50	0.12	0.27	50	0.75	1.51	50	0.22	0.12
100	0.09	0.18	100	0.42	0.83	100	0.55	0.47

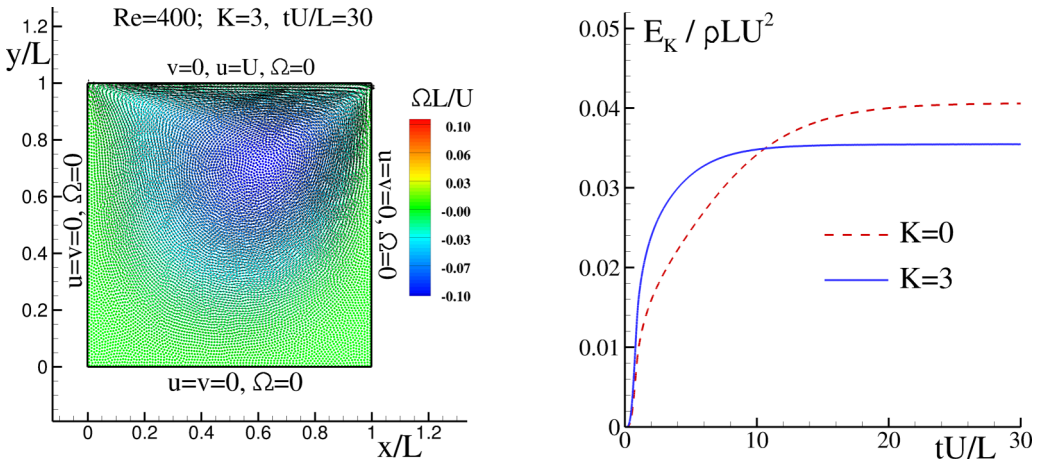

FIG. 4. Lid-driven cavity. Left: Sketch of the problem and of the boundary conditions. Right: time histories of the kinetic energy for $K = 0$ and $K = 3$. The spatial resolution is $N = L/\Delta r = 400$.

rate observed in standard fluid simulations. For ($\mu_r/\mu = 2, a = 2$) both relative errors increase for the finest resolution but remain below 1%.

C. Lid-driven cavity with a micropolar fluid

The lid-driven cavity is a well-known benchmark case for validating numerical solvers on viscous flows. Its physical characteristics resemble those typical of lubrication processes, a field in which micropolar fluids have received great attention in the literature (see, e.g., Refs. [23,24,54]).

In 2012 Chen *et al.* [55] showed numerical simulations of a lid-driven cavity with a micropolar fluid. Since they did simulations for a limited range of parameters and since no velocity profiles were provided, their study is not suitable for validation purposes. More recently, Venkatadri *et al.* [49] studied the same problem providing the velocity profiles, which makes their study adequate for a 2D validation of the present SPH scheme.

Venkatadri *et al.* [49] adopted the momentum Eq. (53) for modeling this problem. They studied the influence of selecting different values of $K = \kappa/\mu$ on the lid-driven cavity flow. Here, for the sake of brevity the cases $K = 0$ (that is standard Newtonian fluid) and $K = 3$ are treated with the proposed SPH model.

In the left panel of Fig. 4 the setup of the problem is shown along with the conditions on the walls. The Reynolds number is $\mathrm{Re} = \rho UL/\mu = 400$ and the spatial resolution is $N = L/\Delta r = 400$ where Δr is the initial particle distance. The right panel of the same figure displays the time history of the kinetic energy for $K = 0$ and $K = 3$. In this latter case, we observe a decrease of the kinetic energy at the steady state, as a consequence of an increase of dissipation due to the spin.

In Fig. 5 the streamlines for the two selected cases are shown. For $K = 3$, a positive vertical displacement of the central vortex is visible, as well as a mitigation of the recirculation vortex at the bottom right corner.

Finally, Fig. 6 shows the comparison between the midsection velocity profiles as predicted by the present SPH model, by the finite difference schemes in Venkatadri *et al.* [49] and by the classic reference of Ghia *et al.* [56] for the Newtonian case. As can be appreciated, the SPH simulation is in qualitative fair agreement with the reference results of the referred Eulerian schemes.

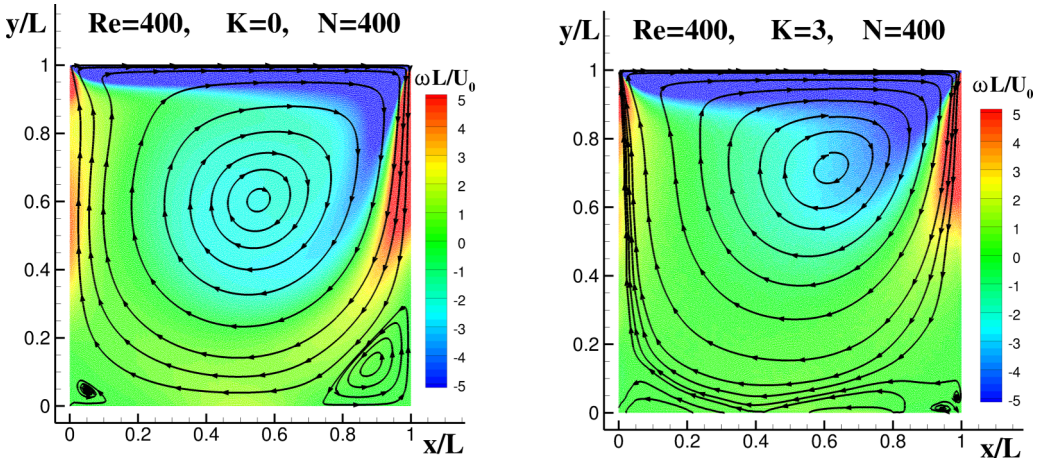

FIG. 5. Lid-driven steady-state streamlines for $\mathrm{Re} = 400$, $\mu_r/\mu = 0$ (left), and $\mu_r/\mu = 2$ (right).

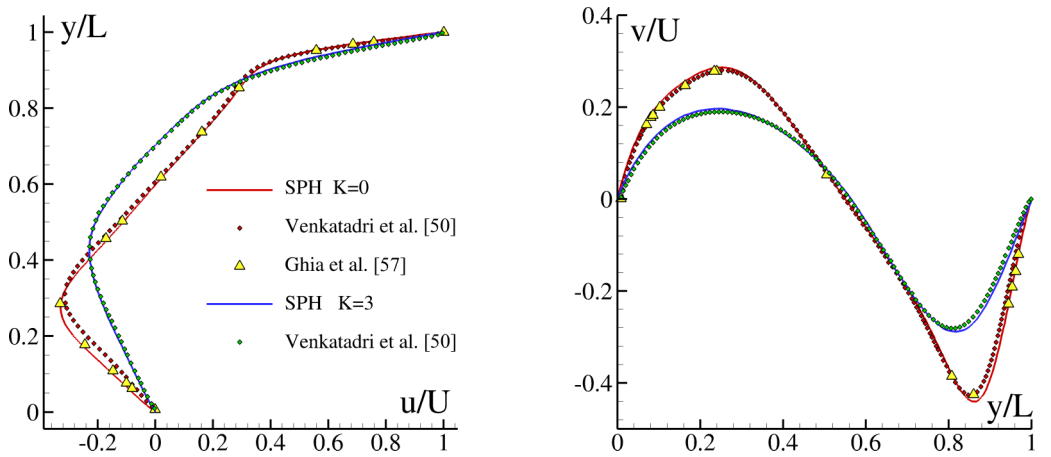

FIG. 6. Lid-driven cavity. Steady-state midsection velocity profiles for Re = 400. Left: horizontal velocity component. Right: vertical velocity component.

VI. CONCLUSIONS

In this paper we have extended the previous bottom-up approaches [16,17] to construct a smoothed particle hydrodynamics (SPH) model to describe the hydrodynamic behavior of general micropolar fluids, with emphasis on their dissipation mechanisms. To this aim, a dissipation function has been defined at the particle level which depends on the relative velocity between particles but also on an additional spin degree of freedom, which modifies such relative velocity and introduces spin-related intrinsic dissipation mechanisms, comparable to those related to the rate of deformation tensor in Newtonian fluids. This dissipation function is invariant under translations and solid-body rotations, which ensures that the resulting forces and torques will respect the conservation of the total momentum and angular momentum of the system. The dissipative forces derived from the dissipation function have been then incorporated to balance the expression obtained from the minimization of the Lagrangian of the system, leading to a set of SPH particle equations to describe the dynamics. The bottom-up approach has also allowed us to discuss in depth the nature of the moment of inertia per unit of mass of the SPH particles.

The obtained discrete model has been taken to the continuum and compared with micropolar models from the literature, establishing the corresponding relationships between their coefficients and the ones of the dissipative terms considered at the particle level.

The developed discrete model has been enriched with additional terms based exclusively on the spin derivatives that were not present in previous SPH models, and that have been obtained with the same bottom-up approach.

Finally, numerical verification (micropolar Poiseuille flow) and validation (micropolar lid-driven cavity) tests have been documented that show that SPH is capable of accurately modeling this type of dynamics.

Future work will include using the developed scheme for problems dealing with micropolar fluids in which the SPH method can be competitive, such as those involving free-surface flows and/or complex physics.

ACKNOWLEDGMENTS

The research activity was partially developed within the Project Area Applied Mathematics of the Department of Engineering, ICT and Technology for Energy and Transport (DIITET) of the Italian National Research Council (CNR). J.B.A. thanks the Ministerio de Ciencia, Innovación y Universidades (MCIU), of the Spanish Government for financial support, Grant No. CTQ2017-84998-P, "Segregación molecular a múltiples escalas en sistemas no tensioctivos para la obtención de materiales avanzados." A.S.I. acknowledges the support of MCIU under Grant No. RTI2018-096791-B-C21, "Hidrodinámica de elementos de amortiguamiento del movimiento de aerogeneradores flotantes."

APPENDIX A: CONTRIBUTIONS TO THE ENTROPY PRODUCTION

The terms in Eq. (28) can be expanded to give

$$
\begin{aligned}
-\sum_i \left[\boldsymbol{f}_i^v\cdot\boldsymbol{u}_i+\boldsymbol{q}_i^v\cdot\boldsymbol{\Omega}_i\right] &= \zeta_1\sum_{i,j\neq i}F(r_{ij})(\boldsymbol{u}_{ij}\cdot\boldsymbol{e}_{ij})(\boldsymbol{e}_{ij}\cdot\boldsymbol{u}_i)\,V_iV_j\\
&+\zeta_2\sum_{i,j\neq i}F(r_{ij})(\boldsymbol{u}_{ij}\cdot\boldsymbol{u}_i)V_iV_j-\zeta_2\sum_{i,j\neq i}F(r_{ij})(\overline{\boldsymbol{\Omega}}_{ij}\times\boldsymbol{r}_{ij})\cdot\boldsymbol{u}_iV_iV_j\\
&-\frac{\zeta_2}{2}\sum_{i,j\neq i}F(r_{ij})\boldsymbol{\Omega}_i\cdot(\boldsymbol{r}_{ij}\times\boldsymbol{u}_{ij})+\frac{\zeta_2}{2}\sum_{i,j\neq i}F(r_{ij})\boldsymbol{\Omega}_i\cdot[\boldsymbol{r}_{ij}\times(\overline{\boldsymbol{\Omega}}_{ij}\times\boldsymbol{r}_{ij})]V_iV_j. \qquad \text{(A1)}
\end{aligned}
$$

Let us analyze each one of them:

$$\{1\} = \zeta_1 \sum_{i,j\neq i} F(r_{ij})(\boldsymbol{u}_{ij}\cdot\boldsymbol{e}_{ij})(\boldsymbol{e}_{ij}\cdot\ \boldsymbol{u}_i)V_iV_j = \zeta_1 \sum_{i,j<i}(\cdot) + \zeta_1 \sum_{i,j>i}(\cdot) = \zeta_1 \sum_{i,j<i}(\cdot) + \zeta_1 \sum_{j,i<j}(\cdot). \tag{A2}$$

We can rename the indices in the second summation:

$$\{1\} = \zeta_1 \sum_{i,j<i} F(r_{ij})(\boldsymbol{u}_{ij}\cdot\boldsymbol{e}_{ij})(\boldsymbol{e}_{ij}\cdot\ \boldsymbol{u}_i)V_iV_j + \zeta_1 \sum_{i,j<i} F(r_{ji})(\boldsymbol{u}_{ji}\cdot\boldsymbol{e}_{ji})(\boldsymbol{e}_{ji}\cdot\ \boldsymbol{u}_j)V_jV_i. \tag{A3}$$

Since $F(r_{ji}) = F(r_{ij})$, $\boldsymbol{u}_{ij} = \boldsymbol{u}_i - \boldsymbol{u}_j = -\boldsymbol{u}_{ji}$, and $\boldsymbol{e}_{ij} = -\boldsymbol{e}_{ji}$, one can write:

$$\{1\} = \zeta_1 \sum_{i,j<i} F(r_{ij})(\boldsymbol{u}_{ij}\cdot\boldsymbol{e}_{ij})^2V_iV_j. \tag{A4}$$

As for the second term, a similar arrangement leads to

$$\{2\} = \zeta_2 \sum_{i,j<i} F(r_{ij})(\boldsymbol{u}_{ij})^2V_iV_j. \tag{A5}$$

The third term is a crossed one between spin and velocity:

$$\{3\} = -\zeta_2 \sum_{i,j\neq i} F(r_{ij})(\overline{\boldsymbol{\Omega}}_{ij}\times\boldsymbol{r}_{ij})\cdot\boldsymbol{u}_iV_iV_j = \zeta_2 \sum_{i,j<i}(\cdot) + \zeta_2 \sum_{j,i<j}(\cdot). \tag{A6}$$

Renaming indices in the second summand:

$$\{3\} = -\zeta_2 \sum_{i,j<i} F(r_{ij})(\overline{\boldsymbol{\Omega}}_{ij}\times\boldsymbol{r}_{ij})\cdot\boldsymbol{u}_iV_iV_j - \zeta_2 \sum_{i,j<i} F(r_{ji})(\overline{\boldsymbol{\Omega}}_{ji}\times\boldsymbol{r}_{ji})\cdot\boldsymbol{u}_jV_iV_j, \tag{A7}$$

and taking into account that $\overline{\boldsymbol{\Omega}}_{ij} = \overline{\boldsymbol{\Omega}}_{ji}$, one gets

$$\{3\} = -\zeta_2 \sum_{i,j<i} F(r_{ij})(\overline{\boldsymbol{\Omega}}_{ij}\times\boldsymbol{r}_{ij})\cdot\boldsymbol{u}_{ij}V_iV_j. \tag{A8}$$

Term {4} is also crossed:

$$\{4\} = -\frac{\zeta_2}{2} \sum_{i,j\neq i} F(r_{ij})\boldsymbol{\Omega}_i\cdot(\boldsymbol{r}_{ij}\times\boldsymbol{u}_{ij}) = \frac{\zeta_2}{2} \sum_{i,j<i}(\cdot) + \frac{\zeta_2}{2} \sum_{j,i<j}(\cdot). \tag{A9}$$

Renaming indices in the second summand:

$$\{4\} = -\frac{\zeta_2}{2} \sum_{i,j<i} F(r_{ij})\boldsymbol{\Omega}_i\cdot(\boldsymbol{r}_{ij}\times\boldsymbol{u}_{ij}) - \frac{\zeta_2}{2} \sum_{i,j<i} F(r_{ji})\boldsymbol{\Omega}_j\cdot(\boldsymbol{r}_{ji}\times\boldsymbol{u}_{ji}), \tag{A10}$$

and due to the antisymmetry of $\boldsymbol{r}_{ij}$ and $\boldsymbol{u}_{ij}$, one gets

$$\{4\} = -\zeta_2 \sum_{i,j<i} F(r_{ij})\overline{\boldsymbol{\Omega}}_{ij}\cdot(\boldsymbol{r}_{ij}\times\boldsymbol{u}_{ij}) = -\zeta_2 \sum_{i,j<i} F(r_{ij})(\overline{\boldsymbol{\Omega}}_{ij}\times\boldsymbol{r}_{ij})\cdot\boldsymbol{u}_{ij}V_iV_j = \{3\}. \tag{A11}$$

Therefore,

$$\{3\} + \{4\} = -2\zeta_2 \sum_{i,j<i} F(r_{ij})(\overline{\boldsymbol{\Omega}}_{ij}\times\boldsymbol{r}_{ij})\cdot\boldsymbol{u}_{ij}V_iV_j. \tag{A12}$$

Term {5} is only on spin:

$$\{5\} = \frac{\zeta_2}{2} \sum_{i,j\neq i} F(r_{ij})\boldsymbol{\Omega}_i\cdot[\boldsymbol{r}_{ij}\times(\overline{\boldsymbol{\Omega}}_{ij}\times\boldsymbol{r}_{ij})]V_iV_j. = \frac{\zeta_2}{2} \sum_{i,j<i}(\cdot) + \frac{\zeta_2}{2} \sum_{j,i<j}(\cdot). \tag{A13}$$

Renaming indices in the second summand:

$$\{5\} = \frac{\zeta_2}{2} \sum_{i,j<i} F(r_{ij})\boldsymbol{\Omega}_i\cdot[\boldsymbol{r}_{ij}\times(\overline{\boldsymbol{\Omega}}_{ij}\times\boldsymbol{r}_{ij})]V_iV_j + \frac{\zeta_2}{2} \sum_{i,j<i} F(r_{ji})\boldsymbol{\Omega}_j\cdot[\boldsymbol{r}_{ji}\times(\overline{\boldsymbol{\Omega}}_{ji}\times\boldsymbol{r}_{ji})]V_iV_j. \tag{A14}$$

Taking into account the symmetry properties already used in previous terms, one gets:

$$\{5\} = \zeta_2 \sum_{i,j<i} F(r_{ij})\overline{\boldsymbol{\Omega}}_{ij}\cdot[\boldsymbol{r}_{ij}\times(\overline{\boldsymbol{\Omega}}_{ij}\times\boldsymbol{r}_{ij})]V_iV_j. \tag{A15}$$

Using the properties of the mixed product, one gets

$$\{5\} = \zeta_2 \sum_{i,j<i} F(r_{ij})(\overline{\boldsymbol{\Omega}}_{ij}\times\boldsymbol{r}_{ij})^2V_iV_j. \tag{A16}$$

Collecting terms 2–5 together, one gets

$$\{2\}+\{3\}+\{4\}+\{5\}=\zeta_2\sum_{i,j<i}F(r_{ij})(\boldsymbol{u}_{ij}-\overline{\boldsymbol{\Omega}}_{ij}\times\boldsymbol{r}_{ij})^2V_iV_j. \tag{A17}$$

Adding them all:

$$\begin{aligned}-\sum_i\left[\boldsymbol{f}_i^v\cdot\boldsymbol{u}_i+\boldsymbol{q}_i^v\cdot\boldsymbol{\Omega}_i\right]&=\zeta_1\sum_{i,j<i}F(r_{ij})(\boldsymbol{u}_{ij}\cdot\boldsymbol{e}_{ij})^2V_iV_j+\zeta_2\sum_{i,j<i}F(r_{ij})(\boldsymbol{u}_{ij}-\overline{\boldsymbol{\Omega}}_{ij}\times\boldsymbol{r}_{ij})^2V_iV_j\\&=\frac{\zeta_1}{2}\sum_{i,j\neq i}F(r_{ij})(\boldsymbol{u}_{ij}\cdot\boldsymbol{e}_{ij})^2V_iV_j+\frac{\zeta_2}{2}\sum_{i,j\neq i}F(r_{ij})(\boldsymbol{u}_{ij}-\overline{\boldsymbol{\Omega}}_{ij}\times\boldsymbol{r}_{ij})^2V_iV_j\\&=\Phi_D,\end{aligned} \tag{A18}$$

as defined in Eq. (9).

APPENDIX B: SPIN EQUATION: RIGHT-HAND SIDE FROM DISCRETE TO CONTINUUM

The term in Eq. (B1) can be approximated by an integral, as $V_i\sim d\boldsymbol{r}$, i.e.,

$$\sum_j F(r_{ij})\boldsymbol{r}_{ij}\times(\overline{\boldsymbol{\Omega}}_{ij}\times\boldsymbol{r}_{ij})V_j \approx\int F(|\boldsymbol{r}-\boldsymbol{r}'|)(\boldsymbol{r}-\boldsymbol{r}')\times\left[\frac{\boldsymbol{\Omega}(\boldsymbol{r})+\boldsymbol{\Omega}(\boldsymbol{r}')}{2}\times(\boldsymbol{r}-\boldsymbol{r}')\right]d\boldsymbol{r}'. \tag{B1}$$

Let us define $\Delta\boldsymbol{r}':=\boldsymbol{r}'-\boldsymbol{r}$. Then, one can propose a multipolar expansion of the fields around the point $\boldsymbol{r}$:

$$\boldsymbol{\Omega}(\boldsymbol{r}')=\boldsymbol{\Omega}(\boldsymbol{r})+\nabla\boldsymbol{\Omega}\cdot\Delta\boldsymbol{r}'+\tfrac{1}{2}\nabla\nabla\boldsymbol{\Omega}:\Delta\boldsymbol{r}'\Delta\boldsymbol{r}'+\ldots. \tag{B2}$$

Due to the fact that the range of the function F within the integral is of $O(h)$ every $\Delta\boldsymbol{r}'$ in the integrand brings a contribution of this order. Therefore, we only have to retain up to first order in the gradient in the expansion in Eq. (B2). Moreover, due to translational invariance, we can write $d\boldsymbol{r}'\to d\Delta\boldsymbol{r}'$. With this, Eq. (B1) can be written as

$$\begin{aligned}&\int F(|\Delta\boldsymbol{r}'|)\Delta\boldsymbol{r}'\times\left[\left(\boldsymbol{\Omega}(\boldsymbol{r})+\frac{1}{2}\nabla\boldsymbol{\Omega}\cdot\Delta\boldsymbol{r}'+\cdots\right)\times\Delta\boldsymbol{r}'\right]d\Delta\boldsymbol{r}'\\&\quad=\int F(|\Delta\boldsymbol{r}'|)\Delta\boldsymbol{r}'\times[\boldsymbol{\Omega}(\boldsymbol{r})\times\Delta\boldsymbol{r}']d\Delta\boldsymbol{r}'+O(h^2).\end{aligned} \tag{B3}$$

The linear term in the gradient of the spin vanishes because we integrate an odd-rank tensor with respect to $\Delta\boldsymbol{r}'$ isotropically. Then, to the lowest order in h we have only the term on the right-hand side of Eq. (B3). Due to the fact that F is of the order of $1/h^3$ [see Eqs. (3) and (4)] the remaining integral is overall of $O(h^0)$ and the neglected corrections are $O(h^2)$.

To carry on the remaining integral, we introduce here the cartesian components of the tensor and index them with Greek letters. Furthermore, we will assume the Einstein convention of implicit summation over repeated indices. Hence, we can write, for the α component:

$$\begin{aligned}&\int F(|\Delta\boldsymbol{r}'|)(\Delta\boldsymbol{r}'\times[\boldsymbol{\Omega}(\boldsymbol{r})\times\Delta\boldsymbol{r}'])_\alpha d\Delta\boldsymbol{r}'\\&\quad=\int F(|\Delta\boldsymbol{r}'|)\varepsilon_{\alpha\beta\gamma}\Delta r_\beta[\varepsilon_{\gamma\mu\nu}\Omega_\mu\Delta r_\nu]d\Delta\boldsymbol{r}'\\&\quad=\int F(|\Delta\boldsymbol{r}'|)(\delta_{\alpha\mu}\delta_{\beta\nu}-\delta_{\alpha\nu}\delta_{\beta\mu})\Delta r_\beta\Omega_\mu\Delta r_\nu d\Delta\boldsymbol{r}'\\&\quad=(\delta_{\alpha\mu}\delta_{\beta\nu}-\delta_{\alpha\nu}\delta_{\beta\mu})\delta_{\beta\nu}\Omega_\mu=2\Omega_\alpha,\end{aligned} \tag{B4}$$

where we have used the fact that the remaining isotropic integral is the identity tensor $\mathbf{1}$, due to the normalization of the kernel W and the definition of F, namely,

$$\begin{aligned}\int d\Delta\boldsymbol{r}'F(\Delta r')\Delta\boldsymbol{r}'\Delta\boldsymbol{r}'&=\frac{4\pi}{3}\mathbf{1}\int_0^\infty d\Delta r'F(\Delta r')(\Delta r')^4\\&=-\frac{4\pi}{3}\mathbf{1}\int_0^\infty d\Delta r'(\Delta r')^3\frac{dW(\Delta r')}{d\Delta r'}\\&=\mathbf{1}.\end{aligned} \tag{B5}$$

Therefore, in the continuous integral limit we have

$$\sum_j F(r_{ij})\boldsymbol{r}_{ij}\times(\overline{\boldsymbol{\Omega}}_{ij}\times\boldsymbol{r}_{ij})V_j\approx 2\boldsymbol{\Omega}+O(h^2) \tag{B6}$$

■

APPENDIX C: PHYSICAL MEANING OF THE MOMENT OF INERTIA PER UNIT OF MASS $\mathcal{I}$

A discussion with regards to the physical meaning of the left-hand side of Eq. (45), as well as on the value of the moment of inertia per unit of mass $\mathcal{I}$ is in order. To address this problem, we have to consider that the SPH particles are in fact coarse-grained lumps of N_α physical particles, the movement of which is summarized into its overall linear and angular momenta. Let us then take all particles in one of these lumps of characteristic size $\Delta r_i\sim V_i^{1/3}$ and index them with Greek letters. The total momentum is then $\boldsymbol{p}_i=\sum_\alpha\boldsymbol{p}_\alpha$, while the total mass is $m_i=\sum_\alpha m_\alpha$. The velocity of the lump is then defined from the relation $\boldsymbol{u}_i=\boldsymbol{p}_i/m_i$. This ratio remains finite in the limit $\Delta r_i\to 0$, provided that there are always many particles inside the lump for the hydrodynamic limit to make physical sense. For the rotational motion we have that the cell angular momentum contains two terms:

$$\boldsymbol{l}_i=\sum_\alpha^{N_\alpha}((\boldsymbol{r}_\alpha-\boldsymbol{r}_i)\times\boldsymbol{p}_\alpha+\boldsymbol{l}_\alpha), \tag{C1}$$

where $\boldsymbol{l}_\alpha$ is the angular momentum of the physical molecules or particles of microscopic size. The first term on the right-hand side of Eq. (C1) is the contribution to the angular

momentum of the SPH particle due to the motion around the lump center, while the second term stands for the angular momentum due to the rotation of the constituent particles around their own center of mass. In analogy with the case of linear momentum, we can define the tensor of inertia per unit of mass of the isotropic, homogeneous lump, $\mathbf{I}_i$, to be such that

$$m_i \mathbf{I}_i = \sum_{\alpha}^{N_\alpha} [m_\alpha (\boldsymbol{r}_\alpha - \boldsymbol{r}_i) \otimes (\boldsymbol{r}_\alpha - \boldsymbol{r}_i) + m_\alpha \boldsymbol{\mathcal{I}}_\alpha], \tag{C2}$$

where $\mathcal{I}_\alpha$ is the intrinsic tensor of inertia of the molecules, per unit of mass. In homogeneous isotropic systems, the tensor of inertia is proportional to the identity matrix $\mathbb{I}$, $m_i \mathbf{I}_i = m_i I_i \mathbb{I}$, with

$$m_i I_i = \sum_{\alpha}^{N_\alpha} [m_\alpha (x_\alpha - x_i)^2 + m_\alpha \mathcal{I}_\alpha], \tag{C3}$$

and the same symmetry is considered for $\boldsymbol{\mathcal{I}}_\alpha$, i.e., $\boldsymbol{\mathcal{I}}_\alpha = \mathcal{I}\mathbb{I}$, where we have assumed that all the molecules are equal and thus dropped α. Again, the rotational velocity of the lump is given by the ratio $\boldsymbol{\Omega}_i = \boldsymbol{l}_i/(m_i I_i)$, which remains finite in the limit $\Delta r_i \to 0$. To develop it further, assuming that the lump is large (it contains many molecules), let us approximate the summation by an integral, i.e.,

$$\sum_{\alpha} m_\alpha \cdots \simeq \int_{V_i} d\boldsymbol{r} \rho \ldots \tag{C4}$$

Then, the right-hand side of Eq. (C3) can be written as

$$m_i I_i \simeq \int_{V_i} d\boldsymbol{r} \rho [|\boldsymbol{r} - \boldsymbol{r}_i|^2 + \mathcal{I}], \tag{C5}$$

Then, dividing both sides of Eq. (C5) by the volume V_i and assuming that the density is nearly constant inside the particle, we have that

$$\rho I_i \simeq c \rho V_i^{2/3} + \rho \mathcal{I}, \tag{C6}$$

where

$$c \equiv \frac{\int_{V_i} d\boldsymbol{r} |\boldsymbol{r} - \boldsymbol{r}_i|^2}{V_i^{5/3}} \tag{C7}$$

is a geometric dimensionless factor of the order of 1 that depends on the geometrical shape of the SPH particle. For example, if we consider homogeneous spheres, then $c \simeq 2/13$, while for cube particles $c = 1/6$. In the general case of a n-dimension fluid, the proper scaling should be of the form

$$I_i = c V_i^{2/n} + \mathcal{I}. \tag{C8}$$

For example, in a bidimensional context with particles having a disk shape we got $c = 1/(2\pi)$ while for squared particles $c = 1/6$. Because of these small differences from the point of view of the simulation the choice of the constant c is not critical, but it can be chosen to better suit the system under scrutiny.

Equation (C8) indicates that the moment of inertia of a SPH simulation of a micropolar fluid depends on the degree of coarse-graining used, due to the fact that the property I_i depends on the volume V_i of the SPH particle. However, as far as the continuum limit leading to Eq. (45) is concerned, we should take the limit $V_i \to 0$ in Eq. (C8), i.e., $I_i \sim \mathcal{I}$. What Eq. (C8) indicates is that, in taking the continuous limit what remains as moment of inertia *is molecular in nature* or, in other words, is proportional to molecular dimensions. Notice that the same limit taken for the mass, produces a macroscopic property, the mass density, which is independent of such molecular dimensions. Therefore, the ultimate value $\mathcal{I}$ will be vanishingly small in normal fluids and typical applications. For the this reason $\mathcal{I}$ is called microinertia. As pointed-out in Ref. [55], $\mathcal{I}$ is in general of order l^2, being l a hidden length scale, which can be a molecular scale or, in other contexts, the Kolmogorov microscale or the Taylor microscale.

Moreover, it is also interesting to investigate under which conditions the spin inertia is physically relevant for the phenomenology that we aim at describing. From Eqs. (45) and (47), we can estimate the relaxation time of the spin by a dominating balance between the inertia, on the left-hand side, and the second term on the right-hand side, i.e., $\tau = \rho \mathcal{I}/2\mu_r$. If L is a characteristic dimension of the system and U a characteristic velocity of the fluid, then the rotational inertia will be relevant if $\tau U/L \gg 1$. We can rewrite this condition as

$$\tau \frac{U}{L} = \mathrm{Re}^\Omega \gg 1, \quad \mathrm{Re}^\Omega := \frac{\rho U \mathcal{I}}{2\mu_r L}, \tag{C9}$$

where we defined the Reynolds number Re^Ω linked to the spin dynamics. This condition is favored in systems of small size with small μ_r and large ratio $\mathcal{I}/L^2$, e.g., fluids having large particles with a significant $\mathcal{I}$. In this condition it is expected that the rotational relaxation cannot be ignored. Conversely for flow conditions where τ is small, for the explicit time integration of Eq. (43), we need to ensure that the time step Δt is always enough smaller than τ.

To end this analysis, let us consider again Eq. (45). If $\mathcal{I}$ depends on molecular dimensions, it implies that the continuum limit of the micropolar model presented so far has negligible rotational inertia for all these flows with no extreme conditions as the ones expressed in Eq. (C9), in which $\mathcal{I} d\boldsymbol{\Omega}/dt$ is not negligible. For the rest of the cases where such extreme situations do not occur, we can neglect the inertia term in the left-hand side of Eq. (45). Under the latter circumstances the spin of the fluid is enslaved by the vorticity, in the absence of external torques, i.e.,

$$\boldsymbol{\Omega} = \tfrac{1}{2} \nabla \times \boldsymbol{u}. \tag{C10}$$

We discuss the implications of this statement in Sec. III C.

[1] D. Violeau, *Fluid Mechanics and the SPH Method* (Oxford University Press, Oxford, UK, 2012).

[2] D. J. Price, J. Comput. Phys. **231**, 759 (2012).

[3] F. Macià, J. M. Sánchez, A. Souto-Iglesias, and L. M. González, Int. J. Numer. Methods Fluids **69**, 509 (2012).

[4] A. Colagrossi, M. Antuono, A. Souto-Iglesias, and D. Le Touzé, Phys. Rev. E **84**, 026705 (2011).

[5] A. Colagrossi, A. Souto-Iglesias, M. Antuono, and S. Marrone, Phys. Rev. E **87**, 023302 (2013).

[6] D. Violeau and B. D. Rogers, J. Hydraul. Res. **54**, 1 (2016).

[7] J. Fang, R. G. Owens, L. Tacher, and A. Parriaux, J. Non-Newtonian Fluid Mech. **139**, 68 (2006).

[8] M. Hashemi, R. Fatehi, and M. Manzari, J. Non-Newtonian Fluid Mech. **166**, 1239 (2011).

[9] A. Vázquez-Quesada, M. Ellero, and P. Español, Microfluid. Nanofluid. **13**, 249 (2012).

[10] A. Vázquez-Quesada and M. Ellero, J. Non-Newtonian Fluid Mech. **167-168**, 1 (2012).

[11] M. Ellero, M. Kröger, and S. Hess, J. Non-Newtonian Fluid Mech. **105**, 35 (2002).

[12] R. Shamsoddini, M. Sefid, and R. Fatehi, J. Mech. Sci. Technol. **30**, 307 (2016).

[13] S. Litvinov, M. Ellero, X. Hu, and N. A. Adams, Phys. Rev. E **77**, 066703 (2008).

[14] M. Ellero, *Advanced Particle-Based Techniques for Complex Fluids and Multiscale Flow Processes* (Springer International Publishing, Cham, 2020), pp. 361–392.

[15] K. Muller, D. A. Fedosov, and G. Gompper, Med. Eng. Phys. **38**, 2 (2016).

[16] A. Colagrossi, D. Durante, J. Bonet Avalos, and A. Souto-Iglesias, Phys. Rev. E **96**, 023101 (2017).

[17] J. B. Avalos, M. Antuono, A. Colagrossi, and A. Souto-Iglesias, Phys. Rev. E **101**, 013302 (2020).

[18] V. Stokes, *Theories of Fluids with Microstructure: An Introduction* (Springer, Berlin, 2012).

[19] J. J. Monaghan and R. A. Gingold, J. Comput. Phys. **52**, 374 (1983).

[20] G. Lukaszewicz, *Micropolar Fluids: Theory and Applications*, Modeling and Simulation in Science, Engineering and Technology (Birkhäuser, Boston, 2012).

[21] D. W. Condiff and J. S. Dahler, Phys. Fluids **7**, 842 (1964).

[22] A. C. Eringen, J. Math. Mech. **16**, 1 (1966).

[23] T. Ariman, M. Turk, and N. Sylvester, Int. J. Eng. Sci. **12**, 273 (1974).

[24] S. Das and S. K. Guha, Industr. Lubricat. Tribol. **71**, 31 (2019).

[25] M. A. Kanso, J. H. Piette, J. A. Hanna, and A. J. Giacomin, Phys. Fluids **32**, 113101 (2020).

[26] J. Bender, D. Koschier, T. Kugelstadt, and M. Weiler, in *Proceedings of the ACM SIGGRAPH/Eurographics Symposium on Computer Animation (SCA '17)*, edited by S. N. Spencer, B. Thomaszewski, and Y. Kangkang (ACM, New York, 2017).

[27] J. Bender, D. Koschier, T. Kugelstadt, and M. Weiler, IEEE Trans. Vis. Comput. Graph **25**, 2284 (2019).

[28] Y. Xu, X. Ban, Y. Peng, X. Wang, S. Liu, and J. Zhou, in *Cooperative Design, Visualization, and Engineering*, edited by Y. Luo (Springer International Publishing, Cham, 2019), pp. 254–260.

[29] S. Liu, X. Wang, X. Ban, Y. Xu, J. Zhou, and Y. Zhang, IEEE Conf. Virt. Reality 3D User Interf. **1**, 1048 (2019).

[30] X. Wang, S. Liu, X. Ban, Y. Xu, J. Zhou, and C. Wang, in *Proceedings of the SIGGRAPH Asia Technical Briefs (SA'19)* (ACM, New York, NY, 2019), pp. 95–98.

[31] K. Müller, D. A. Fedosov, and G. Gompper, J. Comput. Phys. **281**, 301 (2015).

[32] P. Español, Phys. Rev. E **57**, 2930 (1998).

[33] J. P. Morris, P. J. Fox, and Y. Zhu, J. Comput. Phys. **136**, 214 (1997).

[34] A. J. Simmons and D. M. Burridge, Mon. Weather Rev. **109**, 758 (1981).

[35] M. Yang, M. Theers, J. Hu, G. Gompper, R. G. Winkler, and M. Ripoll, Phys. Rev. E **92**, 013301 (2015).

[36] F. Becattini, F. Piccinini, and J. Rizzo, Phys. Rev. C **77**, 024906 (2008).

[37] X. Hu and N. A. Adams, Phys. Fluids **18**, 702 (2006).

[38] D. Violeau, Phys. Rev. E **80**, 036705 (2009).

[39] D. J. Price, J. Wurster, T. S. Tricco, C. Nixon, S. Toupin, A. Pettitt, C. Chan, D. Mentiplay, G. Laibe, S. Glover *et al.*, Pub. Astron. Soc. Aust. **35**, e031 (2018).

[40] P. Español and M. Revenga, Phys. Rev. E **67**, 026705 (2003).

[41] D. Violeau and T. Fonty, Comput. Fluids **191**, 104240 (2019).

[42] J. P. Hansen and I. R. McDonald, *Theory of Simple Liquids*, 2nd ed. (Academic Press, London, 1991).

[43] S. Mas-Gallic and P. A. Raviart, Numer. Math. **51**, 323 (1987).

[44] N. J. Quinlan, M. Lastiwka, and M. Basa, Int. J. Numer. Methods Eng. **66**, 2064 (2006).

[45] R. Di Lisio, E. Grenier, and M. Pulvirenti, Comput. Math. Appl **35**, 95 (1998).

[46] M. Doi, J. Phys.: Condens. Matter **23**, 284118 (2011).

[47] J. Monaghan, Annu. Rev. Astron. Astrophys. **30**, 543 (1992).

[48] R. Aris, *Vectors, Tensors, and the Basic Equations of Fluid Mechaniscs*, Dover Books on Mathematics Series (Dover Publications, Mineola, New York, 1989).

[49] K. Venkatadri, S. Maheswari, C. V. Lakshmi, and V. R. Prasad, IOP Conf. Ser.: Mater. Sci. Eng. **402**, 012168 (2018).

[50] G. Ahmadi, Int. J. Eng. Sci. **14**, 639 (1976).

[51] J. Monaghan, J. Comput. Phys. **159**, 290 (2000).

[52] M. Antuono, P. Sun, S. Marrone, and A. Colagrossi, Comput. Fluids **216**, 104806 (2021).

[53] H. Wendland, Adv. Comput. Math. **4**, 389 (1995).

[54] P. Khatak and H. C. Garg, J. Tribol. **139**, 011707 (2017).

[55] J. Chen, C. Liang, and J. D. Lee, Proc. Inst. Mech. Eng. Part N: J. Nanoeng. Nanosys. **224**, 31 (2010).

[56] U. Ghia, K. N. Ghia, and C. Shin, J. Comput. Phys. **48**, 387 (1982).